


 Cite this: *RSC Adv.*, 2025, 15, 33101

# Synthetic strategies towards preparation and functionalization of ullazines, a promising class of light-harvesting materials

 Thiago J. Peglow,<sup>a</sup> Amanda de A. Borges,<sup>b</sup> Edson Evangelista,<sup>b</sup> Luana da S. M. Forezi<sup>b</sup> and Vanessa Nascimento \*<sup>a</sup>

Polycyclic aromatic hydrocarbons (PAHs) have gained significant attention from the scientific community due to their remarkable optoelectronic properties, which make them ideal candidates for applications in organic electronic materials, such as organic photovoltaics (OPVs) and dye-sensitized solar cells (DSSCs). These compounds, characterized by extended  $\pi$ -conjugation, enable electron delocalization, enhancing their electronic and optical behaviors. The incorporation of heteroatoms in PAHs has been shown to further modify their electronic properties without disrupting the aromaticity, providing additional opportunities for the design of advanced organic semiconductors. A notable example is ullazine, a nitrogen-containing polycyclic system with a 16  $\pi$ -electron structure. It has emerged as a promising material for organic electronics due to its unique electron-donating and electron-accepting capabilities. Recent advances in synthetic methodologies, including metal-catalyzed cyclization and hydride shift reactions, have enabled the development of ullazine derivatives with tunable electronic properties. Furthermore, the inclusion of heteroatoms such as boron and sulfur and the expansion of the ullazine framework through mono- and bis-annulation strategies have enhanced the charge transport properties and light-harvesting capabilities of these compounds, making them highly attractive for photovoltaic applications. This review comprehensively discusses the latest synthetic strategies for ullazine derivatives, their electronic and optical properties, and their potential applications in next-generation organic electronic devices.

 Received 19th May 2025  
 Accepted 19th August 2025

DOI: 10.1039/d5ra03527a

[rsc.li/rsc-advances](http://rsc.li/rsc-advances)

<sup>a</sup>SupraSelen Laboratory, Departamento de Química Orgânica, Universidade Federal Fluminense – UFF, Niterói, Rio de Janeiro, 24020-141, Brazil. E-mail: [nascimentovanessa@id.uff.br](mailto:nascimentovanessa@id.uff.br)

<sup>b</sup>Laboratório de Síntese Orgânica Aplicada, Departamento de Química Orgânica, Universidade Federal Fluminense – UFF, Niterói, Rio de Janeiro, 24020-141, Brazil


**Thiago J. Peglow**

Graduated in Industrial Chemistry from the Universidade Federal de Pelotas, where he obtained his PhD in 2021 under supervision of Prof. Dr Gelson Perin, focusing on green chemistry and synthesis of heterocycles with organochalcogen compounds. He completed a postdoctoral fellowship at the Universidade Federal do Rio Grande do Sul, working with photocatalysis in organic synthesis and the development of new fluorophores, supervised by Prof. Dr Paulo Schneider. Since 2023, he has been a postdoctoral researcher at the Universidade Federal Fluminense, under the supervision of Prof. Vanessa Nascimento, studying green protocols, and synthesis of  $\pi$ -conjugated molecules with optoelectronic potential.


**Amanda de A. Borges**

Received a master's in chemistry (2023) from the Universidade Federal Fluminense (CAPES 6) and a bachelor's degree in chemistry from Universidade Federal Fluminense – UFF (2021), where they developed research projects as a scholarship recipient in the Institutional Program for Technological Development and Innovation Initiation Scholarships – PIBITI (2018–2021) at the Chemistry Institute of Universidade Federal Fluminense, focusing on organic synthesis. Currently, Amanda is a PhD scholarship holder (CNPq) at Universidade Federal Fluminense.



# 1. Introduction

Polycyclic aromatic hydrocarbons (PAHs) have long captured the attention of the scientific community due to their remarkable optoelectronic properties and their pivotal role in organic electronic materials.<sup>1</sup> Their extended  $\pi$ -conjugation facilitates electron delocalization, making them key components in developing organic semiconductors.<sup>2</sup> PAHs are characterized by their extended  $\pi$ -conjugation, which enables unique electronic and optical behaviors, making them highly attractive candidates for applications such as DSSCs and OPVs.<sup>3</sup> Notably, PAHs with embedded heteroatoms (Het-PAHs) offer additional

opportunities for tailoring electronic properties. The introduction of nitrogen atoms in PAHs is particularly appealing due to their ability to modify the electronic structure without disrupting the system's aromaticity.<sup>1</sup> In this context, ullazine, also known as indolizino[6,5,4,3-*ija*] quinoline, is a promising electron-rich heteroaromatic system recently gaining substantial attention in organic electronics.<sup>4</sup> This compound, first synthesized in 1983 by Balli and Zeller, is a 16  $\pi$ -electron nitrogen-containing polycyclic system, isoelectronic to pyrene. Structurally, it can also be seen as a 14  $\pi$ -electron annulene with a positively charged nitrogen resulting from a mesomeric effect, endowing it with both electron-donating and electron-accepting capabilities.<sup>3</sup>

In recent years, synthetic strategies for ullazine and its derivatives have significantly evolved to meet the growing demand for novel organic semiconductors with tunable optoelectronic properties. One of the most promising methodologies involves metal-catalyzed cyclization and hydride shift reactions, which enable the formation of highly conjugated ullazine cores with controlled electronic properties.<sup>5</sup> Additionally, alternative synthetic approaches such as the Friedel–Crafts reaction and [2 + 3] cycloaddition of azomethine ylides have been explored to achieve ullazine synthesis and its subsequent functionalization.<sup>4</sup> The inclusion of heteroatoms such as boron, nitrogen, oxygen, and sulfur within the ullazine framework has enabled fine-tuning of its electronic and optical characteristics.<sup>4</sup> Such N-doped PAHs have demonstrated significant potential in a variety of applications, including light-emitting materials, charge transport layers in organic electronic devices, and dye-sensitized solar cells.<sup>1</sup> The strong electron-donating ability of the ullazine periphery, particularly due to the electron-rich



**Edson Evangelista**

*Obtained a bachelor's degree in chemistry from the Universidade Federal do Recôncavo da Bahia (UFRB), Center for Teacher Education (CFP), Amargosa BA. He was a scholarship holder in teaching initiation through the Institutional Program for Teaching Initiation Scholarships (PIBID/CAPEs). He received his master's and PhD degrees in organic chemistry from the Universidade Federal da Bahia (UFBA), with a focus on organic synthesis. Currently, he is a postdoctoral researcher at the Universidade Federal Fluminense (UFF), working in the research line "Technological Development of Organic Materials for Solar Cells".*

*Obtained a bachelor's degree in chemistry from the Universidade Federal do Recôncavo da Bahia (UFRB), Center for Teacher Education (CFP), Amargosa BA. He was a scholarship holder in teaching initiation through the Institutional Program for Teaching Initiation Scholarships (PIBID/CAPEs). He received his master's and PhD degrees in organic chemistry from the Universidade Federal da Bahia (UFBA), with a focus on organic synthesis. Currently, he is a postdoctoral researcher at the Universidade Federal Fluminense (UFF), working in the research line "Technological Development of Organic Materials for Solar Cells".*



**Luana da S. M. Forezi**

*Graduated in Chemistry from UFJF (2008), with a Master's (2011) and PhD (2014) from UFF, including a sandwich period at the University of Aveiro, Portugal. In 2021, she became a Young Scientist of Our State by FAPERJ, and in 2022, she was recognized as a Young Fluminense Researcher by FAPERJ. In 2023, she was awarded the CNPq Research Productivity Fellowship – PQ2. She is the Regional Vice-Secretary of SBQ-RJ (2024–2026) and a Full Member of Sigma Xi (2024–present). She has coordinated the LabSOA since 2020. Her research focuses on Organic Synthesis. She is the mother of Miguel, who is 3 years old.*

*Graduated in Chemistry from UFJF (2008), with a Master's (2011) and PhD (2014) from UFF, including a sandwich period at the University of Aveiro, Portugal. In 2021, she became a Young Scientist of Our State by FAPERJ, and in 2022, she was recognized as a Young Fluminense Researcher by FAPERJ. In 2023, she was awarded the CNPq Research Productivity Fellowship – PQ2. She is the Regional Vice-Secretary of SBQ-RJ (2024–2026) and a Full Member of Sigma Xi (2024–present). She has coordinated the LabSOA since 2020. Her research focuses on Organic Synthesis. She is the mother of Miguel, who is 3 years old.*



**Vanessa Nascimento**

*Graduated in Industrial Chemistry from Universidade Federal de Santa Maria (2008), completed her PhD in Chemistry at the Universidade Federal de Santa Catarina with a period at UNIPG-Italy (2015). Since 2016, she has been a professor at the Universidade Federal Fluminense, where she leads the group she founded – SupraSelen Laboratory. Her research focuses on the design and synthesis of organochalcogens and macrocycles and their applications. She was Secretary of the Young Researchers of the Brazilian Chemical Society (JP-SBQ), a task group member of the Public Outreach Committee of the IYCN and Regional Treasure of SBQ-RJ. She became a Young Scientist of Our State by FAPERJ fellow (2019–present) and a Young Fluminense Researcher by FAPERJ. She was awarded the CNPq Research Productivity Fellowship – PQ2 (2021 to present) and is an Affiliate Member of the Brazilian Academy of Sciences (2025–2029). She is the mother of Arthur and Lucca, twins of 7 years old.*



pyrrolic nitrogen, has been a crucial factor in the development of high-performance organic semiconductors.<sup>3</sup> Furthermore, substitutions at the 3- and 9-positions of the ullazine core are known to enhance its stability and fine-tune its electronic behavior.<sup>3</sup>

Another key synthetic approach in the field is the use of mono- and bis-annulation strategies to expand the ullazine framework. These techniques, often inspired by established methodologies in polycyclic heteroaromatic chemistry,<sup>2</sup> enable the development of  $\pi$ -extended ullazine derivatives, improving their charge transport properties and broadening their absorption spectra for applications in light-harvesting technologies such as DSSCs and OPVs.<sup>5</sup> Some examples of mono-annulated compounds, which result from a structural modification of the ullazine base, exhibited significantly superior charge transfer properties, highlighting their potential for optoelectronic applications. These mono-annulated systems reveal charge transfer excited states, while the more conjugated closed ullazine derivatives tend to exhibit more apolar photo-physical characteristics.<sup>4</sup>

One of the most promising advances in ullazine chemistry is the use of photochemical cyclodehydrochlorination for synthesizing  $\pi$ -extended derivatives. These metal-free methods enable the development of ullazines fused with electron-donating or electron-deficient groups, improving their light-harvesting and photovoltaic properties. Their extended  $\pi$ -conjugation also promotes self-assembly, enhancing their role in optoelectronic applications. Structural modifications in mono-annulated derivatives improve charge transport and energy conversion compared to traditional ullazines. Additionally, ullazines have shown potential in donor-acceptor conjugated polymers for solar cells, with recent systems achieving power conversion efficiencies (PCEs) up to 2.23%.<sup>1-3,5</sup>

Given the broad range of potential applications of ullazines and their derivatives, as well as the growing interest from the scientific community, this review provides a comprehensive analysis of recent synthetic methodologies for the preparation of ullazine-based compounds. To facilitate clarity and comparison, we classify the synthetic approaches into five main categories: (i) ullazines, (ii) aza-ullazines, (iii) other N-doped ullazines, (iv) BO/BN-doped ullazines, and (v) ullazines fused to other heterocycles (Fig. 1). This classification aims to provide a systematic and in-depth overview of recent advances in the

chemistry of ullazines, with particular emphasis on their synthetic strategies and their potential applications in organic electronic materials, especially in light-harvesting technologies such as DSSCs and OPVs. This manuscript will discuss the latest strategies for designing ullazine-based functional materials and explore their electronic properties, self-assembly behaviors, and their potential for use in next-generation organic photovoltaic devices.<sup>1-5</sup>

## 2. Ullazines

Given the importance of ullazine derivatives, in recent years some synthesis methods of these key compounds have been described in the literature.<sup>6</sup> Among them, methods of annulation using dialkynyl-*N*-(het)arylpyrroles, indium(III)chloride (InCl<sub>3</sub>) as a Lewis acid, and aromatic hydrocarbons as solvents have been highlighted. In 2012, Delcamp and coworkers described the direct annulation of dialkynylarylpyrroles **1** *via* a double cyclization/hydride shift reaction in the presence of catalytic InCl<sub>3</sub> to give the ullazines **2**. These compounds were functionalized at various reactive sites on the ullazine core, which was synthesized in just four scalable steps, with a double Fürstner cyclization serving as the key transformation (Scheme 1). The resulting ullazine derivatives displayed unique electronic properties due to their resonance structures, characterized by a central electron-accepting iminium core and a strongly electron-donating aromatic periphery. This dual nature, along with planar  $\pi$ -conjugation and multiple sites for substitution, facilitated efficient intramolecular charge transfer (ICT). Notably, the dye **3** achieved a power PCE of 8.4% in DSSCs, attributed to its broad light absorption, favorable HOMO-LUMO energy alignment, and stabilized excited-state oxidation potential. The concise synthesis and impressive performance of these ullazine-based sensitizers underscore their strong potential for industrial DSSC applications.<sup>7</sup>

A few years later, there was an exponential growth in studies related to these ullazine derivatives. In 2017, Pierrat and coworkers<sup>8</sup> demonstrated a selective microwave-assisted mono- and bis-annulation of dialkynyl-*N*-(het)arylpyrroles derivatives **12** and **13** promoted by InCl<sub>3</sub>. This protocol also effectively accessed the N-doping structure, giving aza-ullazine derivatives **12d** and **13d** in excellent yields (this class will be addressed during the review). This study was extremely relevant due to selectivity and because it was possible to compare the properties of mono- or bis-annulation products. The mono-annulated systems present interesting charge transfer properties, and these behaviors disappear in the more conjugated bis-annulated ones. This selectivity for obtaining mono- and bis-ullazines was achieved through small changes in the reaction conditions. The reaction optimization studies showed the best reaction condition for the synthesis of mono-annulated derivatives consists of the microwave irradiation of the dialkynyl-*N*-(het)arylpyrroles **11a-c** for 20 minutes using 0.3 equivalent of the catalyst at 90 °C, while for the pyridine derivative **11d** an increase in temperature to 160 °C was necessary to promote annulation (using 2 equiv. of InCl<sub>3</sub>). For the synthesis of bis-annulated derivatives, 1 equiv. of InCl<sub>3</sub> at 130 °C, while for

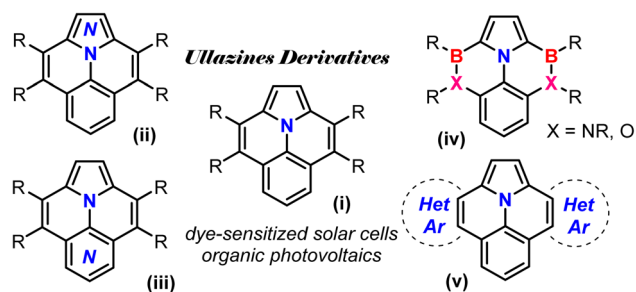
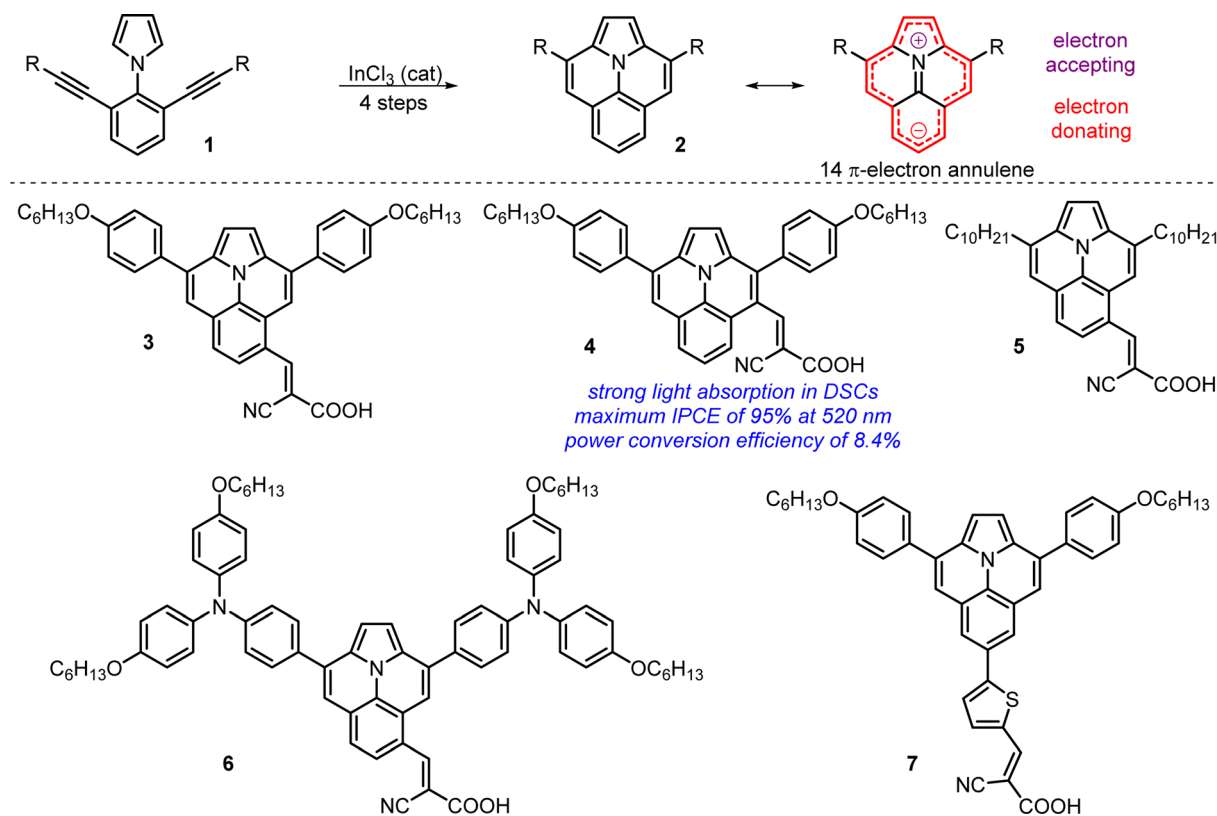


Fig. 1 Classification of ullazines according to their synthetic derivatives.





Scheme 1 Synthesis of ullazine derivatives 3–7.

the pyridine derivative **11d**, 180 °C was necessary to promote annulation (using 3 equiv. of  $\text{InCl}_3$ ).

In general, dialkynyl-*N*-(het)arylpyrroles precursors **11** are synthesized by simple routes (Scheme 2). The first step consists of the bromination reaction that can be carried out *via* electrophilic aromatic substitution ( $\text{S}_{\text{E}}\text{Ar}$ ) using anilines or 4-aminopyridine **8a–c** and *N*-bromosuccinimide (NBS). In the second reaction step, a Clauson–Kaas reaction was performed using 2,5-dimethoxytetrahydrofuran in  $\text{H}_2\text{O}$  or acetic acid under high temperature. In the 3rd step, with substrate **9**, a double Sonogashira cross-coupling reaction was conducted in the presence of the corresponding (het)arylpyrrolyl dibromides **10** and alkynes. The reaction proceeded under microwave irradiation, applying  $\text{PdCl}_2(\text{PPh}_3)_2$  and  $\text{CuI}$  with triphenylphosphine as a catalytic system at 120 °C for 30 minutes, using the mixture of diethylamine and dimethylformamide as solvent. The mono-ringed compounds exhibited intramolecular charge transfer (ICT) properties, making them promising for applications in DSSCs due to their ability to generate polarized excited states and efficient solar energy conversion. In contrast, the bis-ringed systems, though more conjugated, displayed nonpolar photochemical characteristics, limiting their utility in optoelectronic devices. Additionally, protonation of the peripheral nitrogen in aza-ullazine derivatives demonstrated the possibility of further modulating optical properties, reinforcing the potential of these compounds as sensitizers in DSSCs. The study highlights the importance of structural control to optimize the efficiency of organic materials in renewable energy applications.

In the same year, Drigo and coworkers described the synthesis of different ullazine carboxaldehydes through efficient protocols.<sup>9</sup> Initially, the authors carried out the synthesis of the dialkynylarylpyrroles precursors **17a–c** *via* routes b or c (Scheme 3), followed by the annulation step with  $\text{InCl}_3$ , giving the ullazines **18a–c** in good to excellent yields (73–98%).

Next, **18b** was used as a standard substrate for a Vilsmeier–Haack formylation giving different isomeric 3,9-diphenyl-ullazine carboxaldehydes. In this case, there was a limitation in the method, and the corresponding 6-ullazine carboxaldehyde proved to be sensitive to air and oxidized easily when exposed to it, which can be explained by the weak character of electron donation in 6-position. Furthermore, **18b** also provided **19b** in 56% yield, **18c** (2-ullazine-carboxaldehyde) in moderate yield (32%), along with the reported minor product **19d** in 6% yield. This was the first report in the literature for the synthesis of the pyrrole carboxaldehyde **18c** regioisomer (Scheme 4).

In addition, to favor the selective formation of **19d**, not effective in the previously reported protocol, the authors demonstrated a mono-iodoannulation of **17b** promoted by molecular iodine and base, followed by formylation with DMF. Finally, an annulation reaction with  $\text{InCl}_3$  to obtain **19d** in an improved yield of 91% (Scheme 5).

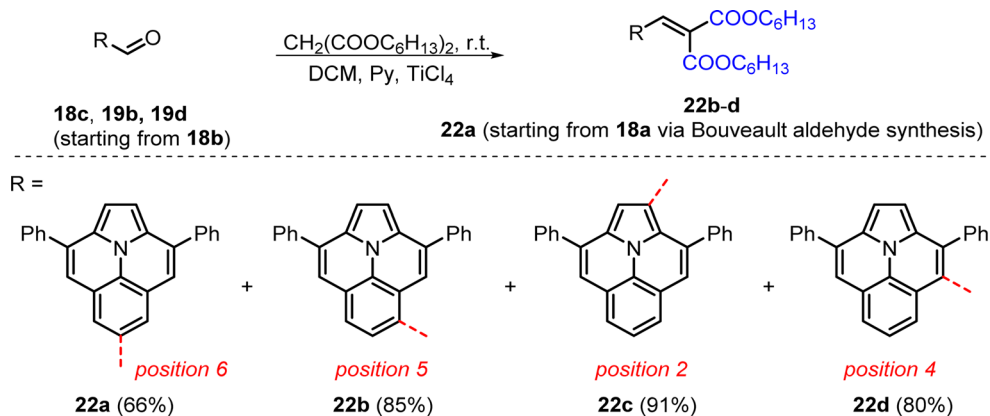
At least, each derivative was subjected to a Knoevenagel condensation to give the respective products **22a–d** in good to excellent yields (66–91%, Scheme 6). In the same work, an ullazine-based dye with an electron-accepting group was tested as a dopant-free hole transport material in a perovskite solar







Scheme 5 Selective synthesis of **19d**. Conditions: (a)  $I_2$ ,  $NaHCO_3$ , DCM, 0 °C; (b)  $nBuLi$ , THF, -78 °C, then dry DMF, -78 °C then r.t.; (c)  $InCl_3$ , toluene, reflux.



Scheme 6 Synthesis of dyes **22a–d**.

using  $InCl_3$ , followed by a Vilsmeier reaction (Scheme 7). However, in this protocol the authors synthesized only the 5-ullazine-carboxaldehyde isomer **25a**, mainly formed in 60% yield. For the structural modification of this derivative, two Wittig–Horner type reactions were described using potassium *tert*-butoxide, followed by a hydrolysis of the esters to give the compounds **26a** and **28a** in a good yield of 75% for both. In addition, to obtain the products **27a**, the compound **25a** was subjected to a Knoevenagel condensation with cyanoacetic acid in the presence of piperidine giving product **27a** in 78% yield. The authors investigate the impact of different anchor groups and  $\pi$ -spacers on the photovoltaic performance of synthesized dyes for DSSCs. As previously described, three dyes (**26**, **27**, and **28**) were synthesized, varying the anchor group (cyanoacrylic acid or carboxylic acid) and the  $\pi$ -spacer (ethylene, phenyl-ethylene, or thiophene-ethylene). **26** featuring cyanoacrylic acid and ethylene, demonstrated the best performance, PCE of 5.28%, due to the strong electron-withdrawing capability of the anchor group and efficient charge transport, resulting in higher light absorption and short-circuit current ( $J_{sc} = 12.28 \text{ mA cm}^{-2}$ ). In contrast, **27** and **28**, with carboxylic groups and longer  $\pi$ -spacers, exhibited blue spectral shifts and reduced efficiencies (1.30% and 1.05%, respectively), attributed to lower electron injection and higher recombination. The study highlights the importance of molecular design, particularly the choice of anchor group and  $\pi$ -spacer, to optimize DSSC efficiency, with **26** emerging as a promising candidate for practical applications.

Along the same path, in 2018, Zhang and coworkers<sup>11</sup> reported new modifications in the structure of these ullazine

derivatives containing alkoxy groups (Scheme 8). In this study, the authors described the synthesis of two isomers containing the formyl group (4-ullazine-carboxaldehyde **32** and 5-ullazine-carboxaldehyde **33**), obtained *via* the Vilsmeier–Haack reaction, with the majority formation of the 4-ullazine-carboxaldehyde **32b** isomer, in 55% yield. These aldehyde derivatives **32** and **33** were reacted with triphenylphosphonium(dibromomethyl)bromide and  $KO^tBu$  *via* a modified Corey–Fuchs reaction to give the respective terminal alkenes **35** and **36**. These derivatives were subjected to a Sonogashira-type cross-coupling with 6-bromo-4,4-dihexyl-4*H*-cyclopenta[2,1-*b*:3,4-*b'*]dithiophene-2-carbaldehyde to give compounds **39a**, **39b**, and **40a** in low to excellent yields. By this method the **40b** derivative was not obtained under similar conditions, therefore, an alternative alkyne-stannylation/Stille coupling route was used to provide the desired **40b** aldehyde in 46% yield. Finally, a Knoevenagel condensation on the resulting aldehydes provided the desired dye series **42** and **43** in 30–97% yields. The authors describe the synthesis and characterization of a series of ullazine-based organic dyes with a donor– $\pi$ –bridge–acceptor (D– $\pi$ –A) structure for application in DSCs. The compounds exhibit uniform panchromatic absorption in the visible region, high PCE up to 5.6%, and potential for light harvesting in near-infrared wavelengths (up to 800 nm). Ullazine, as the donor block, demonstrates unique properties such as strong ICT and redox stability, making these dyes promising for enhancing DSC efficiency. However, challenges such as molecular aggregation in  $TiO_2$  films were identified,





Scheme 7 Synthesis of ullazine carboxaldehydes.

suggesting the need for future molecular design optimizations to maximize photovoltaic performance.

Next, Bao and coworkers<sup>12</sup> described the synthesis of two ullazine-based organic dyes. For this, the authors initially performed a Sonogashira-type cross-coupling reaction followed by a bis-annulation of the dialkynylarylpyrroles precursors **10a** using  $\text{InCl}_3$  in toluene at 100 °C for 24 h (Scheme 9). The unsubstituted ullazine **18b** and *tert*-butyl ullazine **44** were subjected to a Vilsmeier–Haack formylation, giving the 5-ullazine-carboxaldehyde isomer in low yields, followed by a Knoevenagel condensation with cyanoacetic acid in the presence of piperidine giving products **47a** and **47b** in 52% and 8% yields, respectively. These derivatives were applied in  $\text{TiO}_2$ -based nanocrystalline DSSCs, having an overall PCE up to 3.63%.

In 2020, Zhang and coworkers<sup>13</sup> reported the synthesis of a series of symmetrical and unsymmetrical fluorine-rich ullazines. These pentafluorosulfanylated ullazines were synthesized similarly to those described above, *via* bromination, Clauson–Kaas, and Sonogashira reactions (Scheme 10A). However, in this case, to obtain the precursor dialkynylarylpyrroles, the derivatives containing the TMS group were deprotected using base, followed by further Sonogashira coupling with different aryl halides, giving **54a–d** in moderate to good yields (35–85%,

Scheme 10B). Thus, four 4-iodo-ullazines derivatives **55a–d** were obtained *via* bis-annulation of the dialkynylarylpyrroles precursors **54a–d** using  $\text{InCl}_3$  in toluene or 1,2-DCB at high temperature (120–175 °C) for 24 h. Another route proposed by the authors was a mono-iodoannulation reaction of **54b** and **54c** promoted by iodine and base, giving **56a–b**, followed by a cycloaromatization using  $\text{InCl}_3$  to give **57a** and **57b** (58–65%, Scheme 10C). Starting from derivative **56a**, it was still possible to obtain 4-cyano-ullazine **59** over two steps *via* cycloisomerization/substitution (route 1: 45%) or substitution/cycloisomerization (route 2: 60%) approaches (Scheme 10D).

Through route 2 (Scheme 11), the authors also carried out a series of substitutions in the iodine portion of **56a**, giving the mono-ullazine derivatives **60–62**, followed by the final step of cycloaromatization, using  $\text{InCl}_3$ , giving **63–65** in moderate to good yields (42–78%). Furthermore, the compounds **55a–d**, **59** and **63–65** were studied by photophysical, electrochemical, and DFT methods, demonstrating that these symmetrically and unsymmetrically functionalized fluorine-rich ullazines have potential utility in solar energy conversion and other optoelectronic applications.

Next, in 2021, Xia and coworkers<sup>14</sup> reported the synthesis of a series of thienyl functionalized ullazines. For this purpose, in





Scheme 8 Synthesis of dyes 42 and 43.



Scheme 9 Synthesis of two ullazine-based organic dyes.





Scheme 10 Synthesis of unsymmetrical ullazines described in (A–D).

a manner like that described above, the terminal alkynes **66** were reacted with halothiophenes under Sonogashira conditions, followed by cycloaromatization promoted by  $\text{InCl}_3$  in refluxing toluene giving the respective ullazines **69**, **70**, **72a–b**, and **75**. In the case of **75**, thienylation of **66** with 2-(2-ethylhexyl)-5-iodothiophene affords a mixture of **68** and the corresponding

mono-coupling product (4 : 1 ratio) that is difficult to separate and was used in the cycloaromatization step. The derivatives **72a–b** were further subjected to a new coupling reaction using bis(4-methoxyphenyl)amine, giving **73** with three bis-(4-methoxyphenyl)amino donor groups. One of them is directly linked to position 6 of the ullazine core, while the other two are





Scheme 11 Synthesis of unsymmetrical ullazines 63–65.

connected to 3- and 9-positions equivalently by a thienyl ligand. **74** was obtained by coupling with only the methoxylated groups at 3- and 9-positions in the thienyl ring, with 6-position having a methyl group. Likewise, the derivative **75**, containing bromine at 6-position, provided the synthesis of its phenylmethoxylated derivative **76** in 70% yield after 24 h. **75** was further subjected to a Suzuki coupling reaction using pyridin-4-ylboronic acid, Pd(PPh<sub>3</sub>)<sub>4</sub>, K<sub>2</sub>CO<sub>3</sub>, and DMA/H<sub>2</sub>O as solvents at 110 °C, giving the derivative **77** in 65% yield after 8 h (Scheme 12).

A generic scheme of possible modifications on the ullazine scaffold is shown in Scheme 13. Experimental and theoretical analyses have shown that thiophene derivatives with  $-N(p\text{-MeOC}_6\text{H}_4)_2$  groups improve the conductivity of ullazine organic hole-transporting materials (HTMs), increasing the efficiency of PSCs (perovskite solar cells) from about 13.08% to 20.21%. This value is the highest reported to date for ullazine-based HTMs and is close to the performance of spiro-OMeTAD. In addition, unencapsulated PSCs based on the champion ullazine exhibit superior stability concerning spiro-OMeTAD, retaining nearly 90% of the initial efficiency following 1000 h aging, which is ascribed to a combination of higher water repellency and passivation of defects on the perovskite surface.

Alternatively, in addition to the use of InCl<sub>3</sub>, other protocols have been described for the synthesis of ullazines in recent years. In 2016, Wan and coworkers<sup>15</sup> described an efficient method to construct  $\pi$ -conjugated ullazines *via* the palladium-catalyzed direct C–H cyclization of dibromophenylpyrroles **78** with internal alkynes **79**. By this procedure twenty different ullazine derivatives **80a–g** were prepared in moderate to good

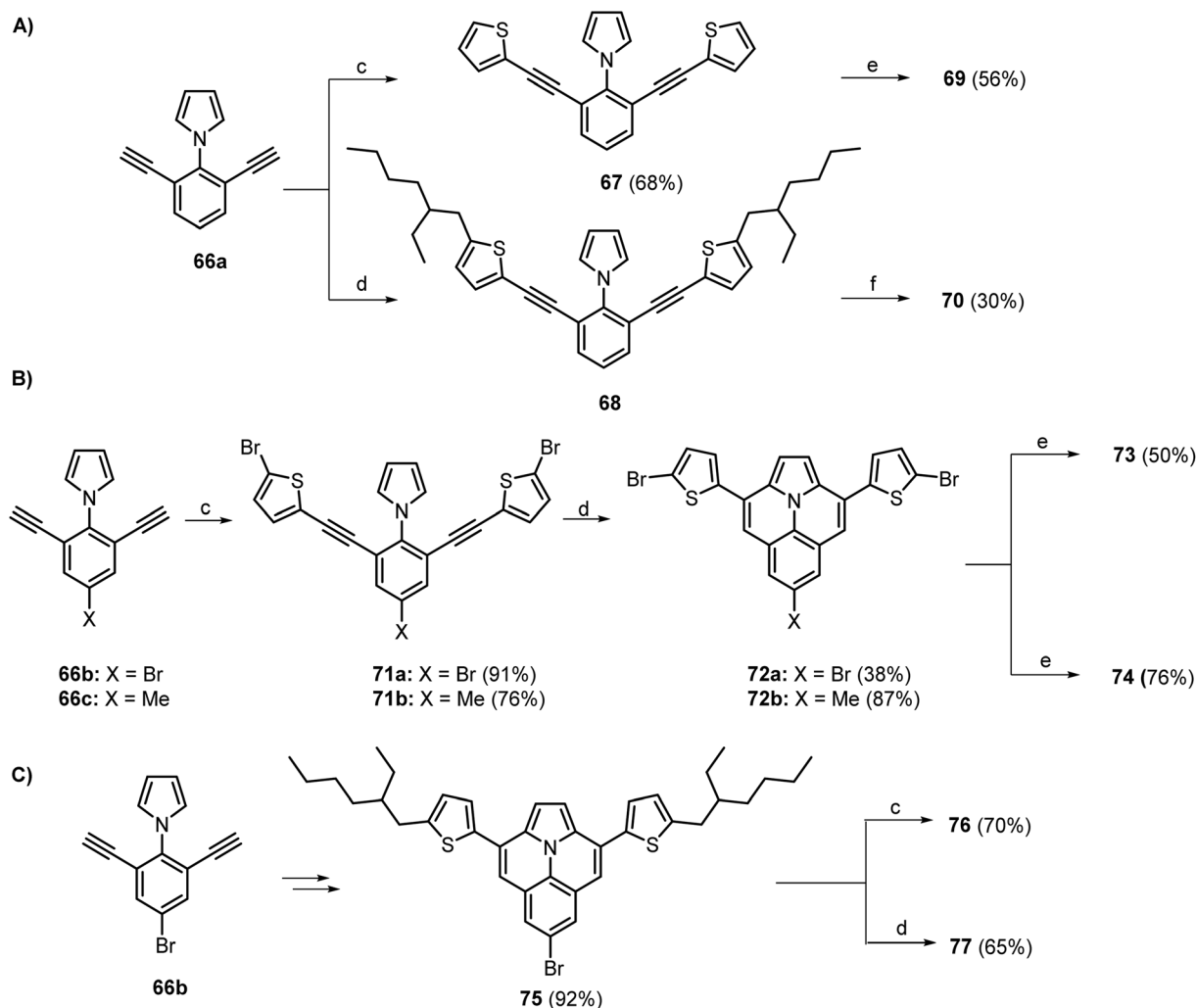
yields (27–80%). This method was compatible with electron-donating groups and electron-withdrawing groups such as alkoxy, chloro, ester, and nitrile (Scheme 14).

The authors proposed a mechanism that begins with the oxidative addition of compound **78a** with Pd(0), forming intermediate **A**. This intermediate then reacts with an alkyne **79a** to produce the palladium(II) complex **B**. The vinylic palladium intermediate **B** undergoes a ring-closing reaction *via* an electrophilic attack on the C-2 position of pyrrole, resulting in the formation of the mono-annulated product **D** after reductive elimination. Subsequent annulation of **D** with an alkyne, following a similar catalytic cycle, gives the desired product **80a** (Scheme 15).<sup>15</sup>

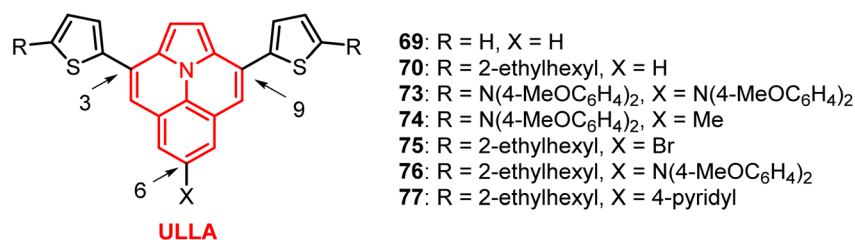
Furthermore, three new ullazine-based sensitizers **83a–c** were obtained from a Vilsmeier–Haack formylation, followed by a Knoevenagel condensation (Scheme 16).<sup>15</sup> The photovoltaic performance of the ullazine-based dyes was evaluated DSSC devices under simulated AM 1.5G illumination. Among them, sensitizer **83c** exhibited the highest power conversion efficiency ( $\eta = 6.1\%$ ), with a short-circuit current density of 9.06 mA cm<sup>-2</sup>, an open-circuit voltage of 0.649 V, and a fill factor of 0.663. The IPCE spectrum of the **83c**-based DSSC revealed a broad response ranging from 300 to 600 nm, reaching a maximum of 70% at 471 nm. These results highlight the strong potential of ullazine derivatives as promising candidates for application in organic optoelectronic materials.

Another route, described by Wang and coworkers<sup>16</sup> was performed to synthesize a series of  $\pi$ -extended dibenzo[*d,k*]-ullazines **85** *via* a double annulation reaction of 1-(2,6-





**Scheme 12** Synthesis of ullazines derivatives. Conditions: (A) (c) 2-bromo-thiophene, Pd(Ph<sub>3</sub>)<sub>4</sub>, Cul, Et<sub>3</sub>N, DMF, 75 °C, 72 h, 68%; (d) 2-(2-ethylhexyl)-5-iodothiophene, Pd(Ph<sub>3</sub>)<sub>4</sub>, Cul, Et<sub>3</sub>N, DMF, 75 °C, 72 h; (e) InCl<sub>3</sub>, toluene, 115 °C, 3 h, 56%; (f) InCl<sub>3</sub>, toluene, 115 °C, 18 h, 30% yield based on 3. (B) (c) 2-Bromo-5-iodothiophene, Pd(Ph<sub>3</sub>)<sub>4</sub>, Cul, Et<sub>3</sub>N, THF, rt, 5 d, 91% (**71a**) or 76% (**71b**); (d) InCl<sub>3</sub>, toluene, 115 °C, 5 h, 38% (**72a**) or 87% (**72b**); (e) bis(4-methoxyphenyl)amine, Pd<sub>2</sub>(dba)<sub>3</sub>, tri-*t*-butylphosphine, NaOtBu, 115 °C, 36 h, 50% (**73**) or 76% (**74**). (C) (c) Bis(4-methoxyphenyl)amine, Pd<sub>2</sub>(dba)<sub>3</sub>, tri-*t*-butylphosphine, NaOtBu, 115 °C, 24 h, 70%; (d) pyridin-4-ylboronic acid, Pd(PPh<sub>3</sub>)<sub>4</sub>, K<sub>2</sub>CO<sub>3</sub>, DMA/H<sub>2</sub>O, 110 °C, 8 h, 65%.



**Scheme 13** Modifications performed on the ullazine scaffold.

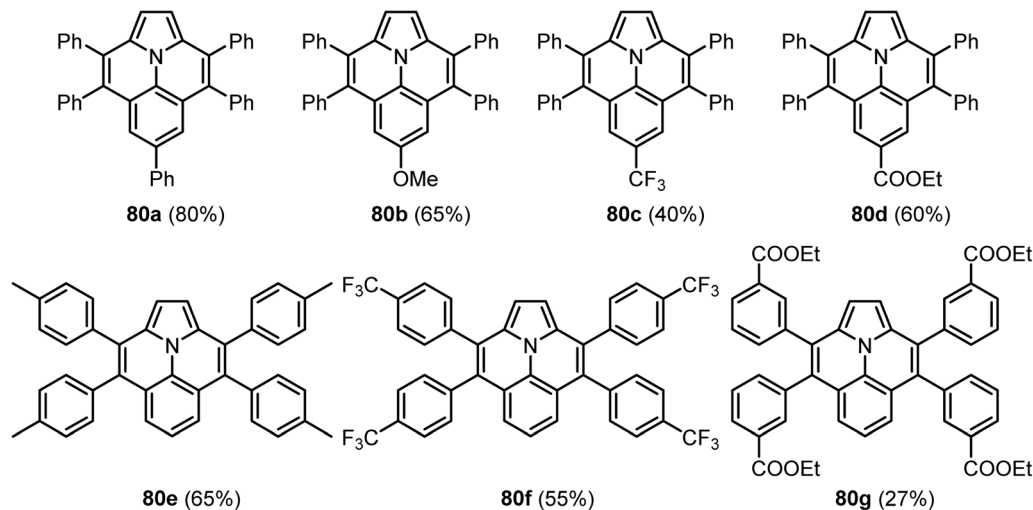
dibromophenyl)-1*H*-pyrroles with arynes (Scheme 17). For this, 2-(trimethylsilyl)aryl trifluoromethanesulfonates **84** were used as the aryne precursors in the presence of Pd(OAc)<sub>2</sub> (10 mol%), dppm (10 mol%), CsF (4.0 equiv.) and Na<sub>2</sub>CO<sub>3</sub> (1.0 equiv.) in MeCN at 100 °C for 24 h in a nitrogen atmosphere. By this

procedure, nineteen different dibenzo[*d,k*]-ullazines were prepared in poor to moderate yields (22–95%). The method was shown to be general and was not sensible to the presence of electron-withdrawing and electron-donor groups attached to the aromatic rings of both the 1-(2,6-dibromophenyl)-1*H*-





Selected examples

Scheme 14 Synthesis of ullazine derivatives **80a–g**.

Scheme 15 Proposed mechanism to form ullazine derivatives described by the authors.

pyrroles and the 2-(trimethylsilyl)aryl trifluoromethanesulfonate.

The mechanism of the synthesis of dibenzo[*d,k*]ullazine derivatives **85** involves an initial oxidative addition of the Pd(0) species with the aryne to generate palladacycle **A**. Next, **A**

reacts with **78a** to form intermediate **B**, which undergoes an intramolecular C–H activation to give the palladacycle **C**, followed by a reductive elimination giving the mono-annulated intermediate **D**. Subsequently, a similar catalytic cycle between **A** and **D** provides the desired product **85a** (Scheme 18).



Scheme 16 Synthesis of ullazine-based sensitizers **83a–c**.Scheme 17 Synthesis of ullazines **85a–g**.

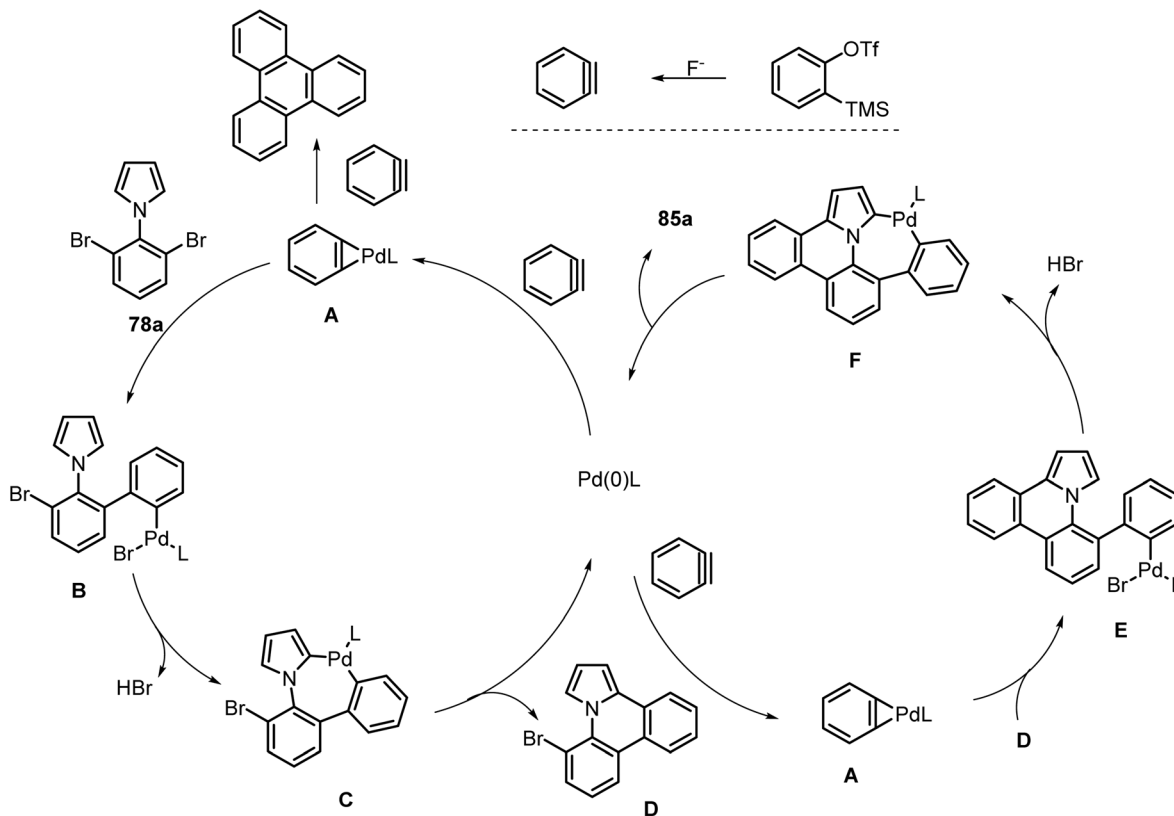
The generation of triphenylene as a byproduct supported this mechanism. However, a pathway that begins with an oxidative addition of the Pd(0) species with **78a** was not ruled out by the authors.<sup>16</sup>

The synthesized compounds, characterized by their planar structure and ICT properties, demonstrate potential applications in functional organic materials, such as DSSCs and organic field-effect transistor (OFETs). Additionally, their

photophysical properties, including tunable fluorescence emission and high quantum yields, suggest utility in optoelectronic devices. The synthesis of the parent dibenzo[*d,k*]-ullazine core, unprecedented until now, paves the way for developing new materials with applications in renewable energy and organic electronics.<sup>16</sup>

A distinct strategy was recently used by Otero-Riesgo coworkers<sup>17</sup> in the synthesis of a range of functionalized





Scheme 18 Mechanism of the synthesis of dibenzo[*d,k*]-ullazine derivatives **85**.

ullazines **88a–g** (Scheme 19). In this protocol, the authors described an one-pot Rh(III)-catalyzed twofold C–H activation/double annulation of *N*-arylpyrroles with diarylalkynes (3.2 equiv.). The reaction was carried out in the presence of RhCp\*(OAc)<sub>2</sub> (10 mol%), Cu(OAc)<sub>2</sub>·H<sub>2</sub>O (220 mol%), in toluene as a solvent at 135 °C under an argon atmosphere. By this protocol, the substrates were converted to the respective ullazines **88** after 72 h in poor to good yields. The reaction tolerates electron-donating group (EDG) and electron-withdrawing group (EWG) substituents on both partners, including halogens, reactive groups in a range of useful reactions.

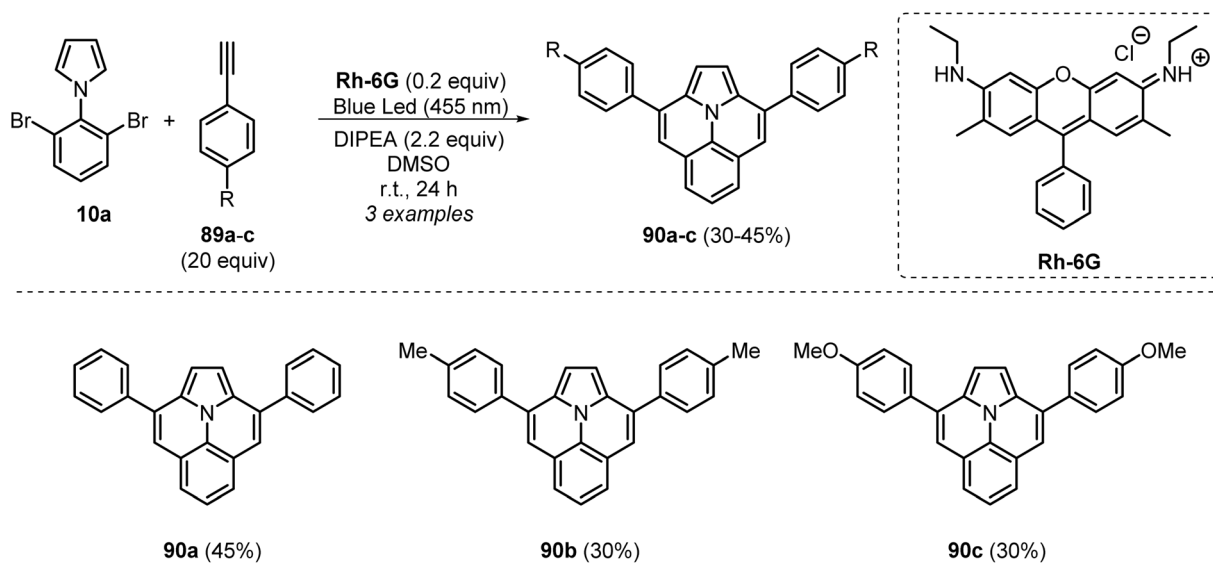
The synthesized compounds exhibit strong fluorescence, with significant bathochromic shifts when substituted with thiophene or triarylamine units, indicating extended electronic properties. These characteristics make the obtained ullazines promising for applications in optoelectronic devices, such as DSSCs and PSCs, where they can act as charge transport materials or light absorbers. Additionally, the ease of further functionalization *via* electrophilic bromination paves the way for targeted modification of these compounds, expanding their potential in advanced materials.

Furthermore, some protocols have been described using visible light and an Rh-based photocatalyst promoting the synthesis of ullazines. The first report was by Das and coworkers,<sup>18</sup> in 2016, using arylpyrrolyl dibromides **10a** e aryl alkynes **89** (Scheme 20). The reaction was performed in the presence of rhodamine 6G (Rh-6G) (0.2 equiv.) and DIPEA (2.2

equiv.), in DMSO at room temperature and under blue LED irradiation. This method provides, in a single step, mild and efficient access to three substituted ullazines bearing neutral and electron-donor substituents in the aromatic ring of the arylalkynes in moderate yields. The synthesized compounds have potential applications in various fields, including pharmacology, due to their antitumor, antibacterial, and apoptosis-inducing activities, as well as in organic materials, such as semiconductors and components for DSSCs. Ullazines, in particular, stand out for their electron-transport properties and optoelectronic applications. The method avoids the use of transition metals and harsh conditions, offering a sustainable and efficient route to obtain these nitrogen-containing heterocycles, which are relevant for both drug development and advanced electronic devices.

Recently, some of us<sup>19</sup> described the selective synthesis of non-symmetrical ullazine **91** (Scheme 21). This protocol consisted of the reaction between the dialkynyl-*N*-arylpyrrole precursor **11b** and indium(III) chloride (3.0 equiv.) using toluene as a solvent under nitrogen atmosphere. The mixture reaction was irradiated under 100 W and blue LED chips, for 24 h at room temperature, giving **91** in 71% yield. The obtained compounds exhibit tunable absorption and emission properties, with significant Stokes shifts and, in some cases, dual emission, suggesting possible complex ICT mechanisms. The synthesized ullazines, obtained *via* selective photocatalysis, demonstrate bathochromic shifts due to increased conjugation,



Scheme 19 Synthesis of a range of functionalized ullazines **88a-g**.Scheme 20 Synthesis of ullazines **90a-c**.

making them promising candidates for DSSCs and OLEDs. Additionally, the structural modularity of these compounds enables the development of materials with tailored electronic properties, potentially applicable in chemical sensors or bioimaging. Theoretical studies corroborate the experimental

data, reinforcing the viability of these systems for advanced applications in photonics and organic electronics.

The synthesis of the ullazine core, as discussed in this review, has been achieved through various methodologies, most notably *via* the cycloaromatization of dialkynyl-*N*-(het)





Scheme 21 Selective synthesis of non-symmetrical ullazine 91.

arylprrrole precursors using indium(III) chloride in aromatic hydrocarbon solvents at elevated temperatures. The reaction afforded mono- or bis-annulated products with high selectivity, governed by the amount of InCl<sub>3</sub> and temperature. In addition to conventional thermal protocols, alternative approaches employing sustainable energy sources have been explored. For instance, Pierrat and coworkers<sup>8</sup> reported a microwave-assisted cycloaromatization that significantly reduced reaction times compared to conventional methods, while Das and coworkers<sup>18</sup> demonstrated a visible-light-promoted synthesis that circumvented the initial Sonogashira cross-coupling step. Although the latter strategy aligned with green chemistry principles, it suffered from prolonged reaction times, narrow substrate scope, and modest yields. In this context, considering the remarkable relevance and distinctive photophysical and electronic properties of non-symmetrical ullazines, some of us<sup>19</sup> dedicated efforts to developing a highly selective synthetic route toward a mono-ullazine derivative. This was accomplished *via* a visible-light-induced annulation of a dialkynyl-*N*-arylprrrole

precursor in the presence of indium(III) chloride, enabling the efficient and sustainable formation of the target scaffold. Furthermore, alternative mono-annulation strategies not reliant on InCl<sub>3</sub> were described by Drigo and coworkers<sup>9</sup> and Zhang and coworkers<sup>13</sup> involving iodine/base-promoted mono-iodoannulation followed by InCl<sub>3</sub>-mediated cycloaromatization. These approaches enabled diverse structural modifications, thereby expanding the library of ullazine derivatives for subsequent photophysical studies.

### 3. Aza-ullazines

As briefly mentioned in some works described above, the possibility of ullazine N-doping can enhance its photophysical properties. Here we describe some additional synthesis protocols solely for aza-ullazine derivatives that were found in the literature. For these pyridine substrates, the methods described usually apply Lewis or Brønsted acids. The first to be mentioned was described in 2017 by Boldt and coworkers,<sup>20</sup> which reports an intramolecular aromatic substitution of dialkynyl-*N*-(het) arylprrrole derivatives **92a–g** promoted by *para*-toluenesulfonic acid (*p*TSA). In this case, some Lewis acids were tested, but the cyclization reactions did not prove to be very efficient. The best condition for this transformation involves stirring a mixture of precursor **92** (1 equiv.) in xylene as solvent in the presence of *p*TSA (35 equiv.) as additive, at 120 °C for 24 h (Scheme 22). Under these conditions, a study on the scope of the reaction was carried out using various electron-rich and electron-deficient substrates, allowing the synthesis of ten 6-aza-ullazines



Examples



Scheme 22 Synthesis of 6-aza-ullazines 93.



analogues in low to excellent yields (16–90%). The reaction was markedly affected by steric hindrance in the presence of an *o*-OMe group, compound **93d**, giving a yield of only 16%. Furthermore, the presence of EWG attached to the aromatic ring of the ethynyl moiety also caused a reduction in the yields to 40 and 30%, respectively. The investigations revealed that these compounds exhibit absorption and emission spectra similar to the parent structure but with a higher oxidation potential, making them potential candidates for application in DSSCs. Thus, aza-ullazines can be explored in innovative electronic devices, particularly in the solar energy sector, due to their ability to stabilize excited states and enhanced electrochemical characteristics.

In a very similar protocol, Janke and coworkers<sup>21</sup> recently described the synthesis of a series of 5-aza-ullazines isomers **95** via *p*TSA-mediated benzannulation of **94** (Scheme 23). Here, the authors used 30 equivalents of *p*TSA and increased the reaction temperature to 140 °C, which allowed reducing the reaction time to 6 h. By this method, thirteen 5-aza-ullazine derivatives containing EWG and EDG linked to the ethynyl moiety were obtained in moderate to excellent yields. It is worth noting that in addition to the arylethynyl precursors, it was possible to use a substrate containing the alkylethynyl moiety, giving the derivatives of interest **95d** and **95h**, although in lower yields (41 and 50%, respectively). The compounds exhibit light absorption and emission in specific ranges, with promising quantum yields (13–43%), along with tunable oxidation and reduction potentials. These characteristics make them attractive candidates for

applications in materials science, such as OLEDs, DSSCs, and OFETs. The modulation of electronic properties through the introduction of nitrogen atoms and additional aromatic rings paves the way for the development of functional materials with potential use in optoelectronic and photovoltaic devices.

Returning to the 6-aza-ullazines isomers, another cyclization route of the dialkynyl-*N*-(het)arylpyrrole precursors was described by Parpart and coworkers<sup>22</sup> via a Friedel–Crafts acylation followed by an intramolecular alkynyl-carbonyl metathesis (ACM) reaction (Scheme 24). In this protocol, the authors reported a synthesis of unsymmetrical aza-ullazines starting from dialkynyl-*N*-(het)arylpyrroles **96**. The trifluoroacetylation reaction was carried out in the presence of trifluoroacetic anhydride (TFAA, 15 equiv.), followed by intramolecular ACM in one step using Cu<sub>2</sub>CO<sub>3</sub>(OH)<sub>2</sub>, K<sub>2</sub>CO<sub>3</sub> and 1,2-dichlorobenzene (DCB) as a solvent at 170 °C for 1 h. The protocol tolerates various substituents on the alkynyl groups. Electron-donating groups, such as 4-methoxyphenyl (**97c**), resulted in excellent yield (96%), whereas electron-withdrawing groups (**97d**) afforded only moderate yield (58%). However, in the case of strongly electron-deficient alkynyl groups (**97e**) or aliphatic alkynes (**97g**), no reaction was observed.

The authors further performed the replacement of TFAA by other electron-efficient anhydrides **99**, giving the desired compounds **100a–d** in good to excellent yields (69–93%) (Scheme 25). The synthesized structures exhibit remarkable optical properties, with absorption maxima around 390 nm and fluorescent emission near 600 nm, along with quantum yields

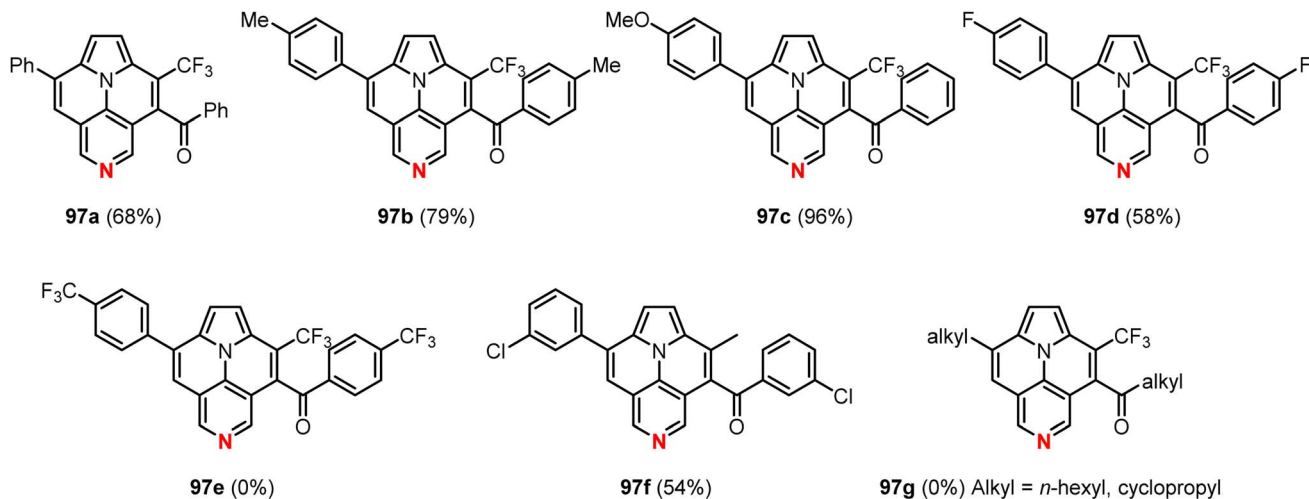
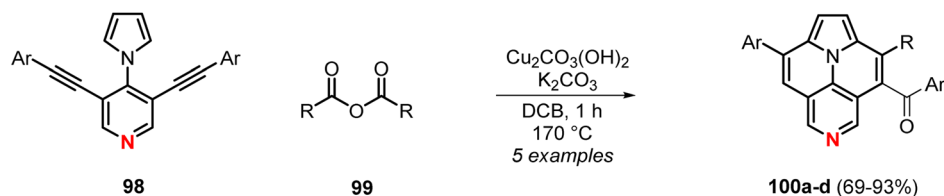


Scheme 23 Synthesis of a series of 5-aza-ullazines **95**.

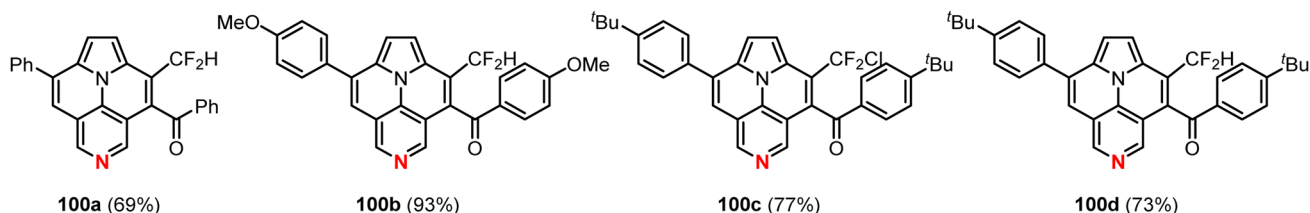




Selected examples

Scheme 24 Synthesis of unsymmetrical aza-ullazines **97**.

Examples

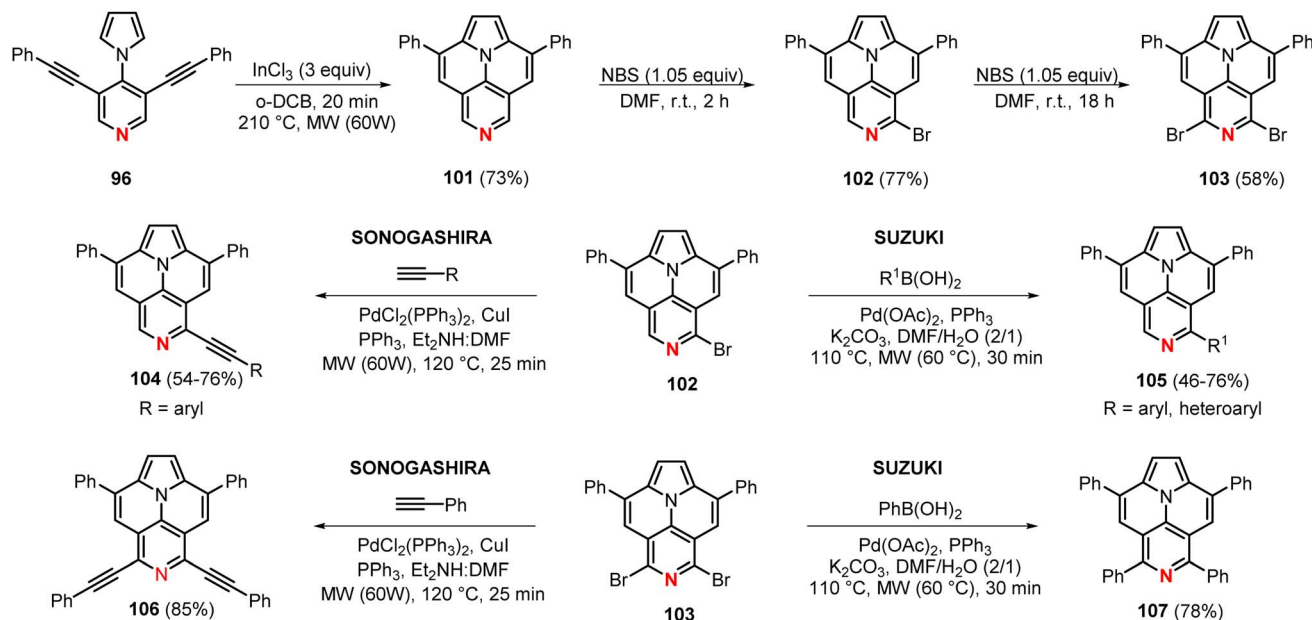
Scheme 25 Synthesis of unsymmetrical aza-ullazines **100**.

of up to 10.4%. These characteristics, combined with the structural modularity enabled by the introduction of aryl or alkyl groups, highlight the potential of these compounds for optoelectronic applications, such as in OLEDs and fluorescent sensors. The versatility of the synthesis and the ability to tune electronic properties make these aza-ullazines promising candidates for the development of new functional materials in photonic and organic electronic devices.

By the same protocol already described above for the synthesis of ullazines, Ibrahim and coworkers<sup>23</sup> performed the

obtention of aza-ullazine **101** using  $\text{InCl}_3$  as Lewis acid. The reaction occurs using a double annulation of the precursor **11d** using an excess of  $\text{InCl}_3$  (3.0 equiv.) under microwave irradiation at 210 °C for 20 min, giving **101** in 73% yield (Scheme 26). Next, a regioselective functionalization of **101** was performed *via* metalation using BuLi-containing aggregates (BuLi-LiDMAE) or electrophilic substitution. According to the authors, this reaction was first described by them, and although direct metalation is an alternative to obtain halogenated derivatives, the yields obtained were relatively low. To overcome





Scheme 26 Synthesis of aza-ullazines 104–107.

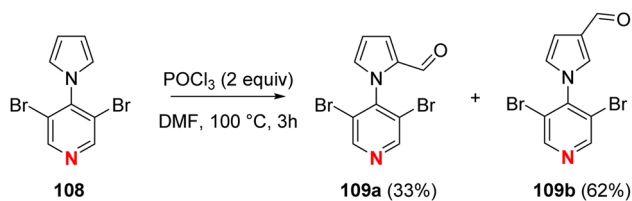
this limitation, the reaction was also performed *via* electrophilic substitution using NBS, leading to mono- and di-brominated compounds **102** and **103** in good to excellent yields. These derivatives were subsequently converted to aryl and alkynyl aza-ullazine derivatives by Suzuki and Sonogashira cross-coupling reactions. The synthesized compounds exhibit promising characteristics for use in dye-sensitized solar cells, OFETs, and other electronic devices, owing to their conjugated structure and tunable properties such as light absorption and emission. This study led to the development of novel functional materials in the field of organic electronics.

In 2024, an efficient synthetic approach for the preparation of quinolino-aza-ullazines was developed by Polkaehn and coworkers,<sup>24</sup> employing a sequential combination of Vilsmeier–

Haack reactions, Sonogashira couplings, Povarov reactions, and cycloisomerizations. The target compounds are diarylindolino [6,5,4,3-*ija*]quinolino[2,3-*c*][1,6]naphthyridines—novel polycyclic structures incorporating electron-donating and electron-withdrawing units arranged to promote intramolecular charge transfer (ICT). The synthesis begins with 3,5-dibromo-4-(1H-pyrrol-1-yl)pyridine, which undergoes double formylation *via* a Vilsmeier–Haack reaction to afford aldehydes **109a** and **109b** (Scheme 27).

Isomer **109a** was used in double Sonogashira couplings with various arylalkynes (Scheme 28), using PdCl<sub>2</sub>(PPh<sub>3</sub>)<sub>2</sub> and cataCXium A as the catalytic system resulting in the compounds **110a–e** in good yields (45–87%).

The compounds **110a–e** were subjected to Povarov reactions with anilines, and FeCl<sub>3</sub> (0.1 equiv.) as the catalyst, followed by a cycloisomerization step using *p*-TsOH (20 equiv.) in xylene (Scheme 29). The methodology was also successfully adapted to a one-pot procedure, eliminating the need for intermediate isolation. Variation of the alkynyl and aniline substituents yielded a library of quinolino-aza-ullazines (**111a–f**) with moderate to good yields (21–65%). The final compounds displayed strong absorption in the visible range, green fluorescence ( $\Phi = 19\text{--}35\%$ ), and features characteristic of ICT and TICT, as demonstrated through solvatochromism, protonation



Scheme 27 Synthesis of 109a,b.



Scheme 28 Synthesis of compounds 110a–e.





## Examples

Scheme 29 Synthesis of quinolino-aza-ullazines **111a-f**.

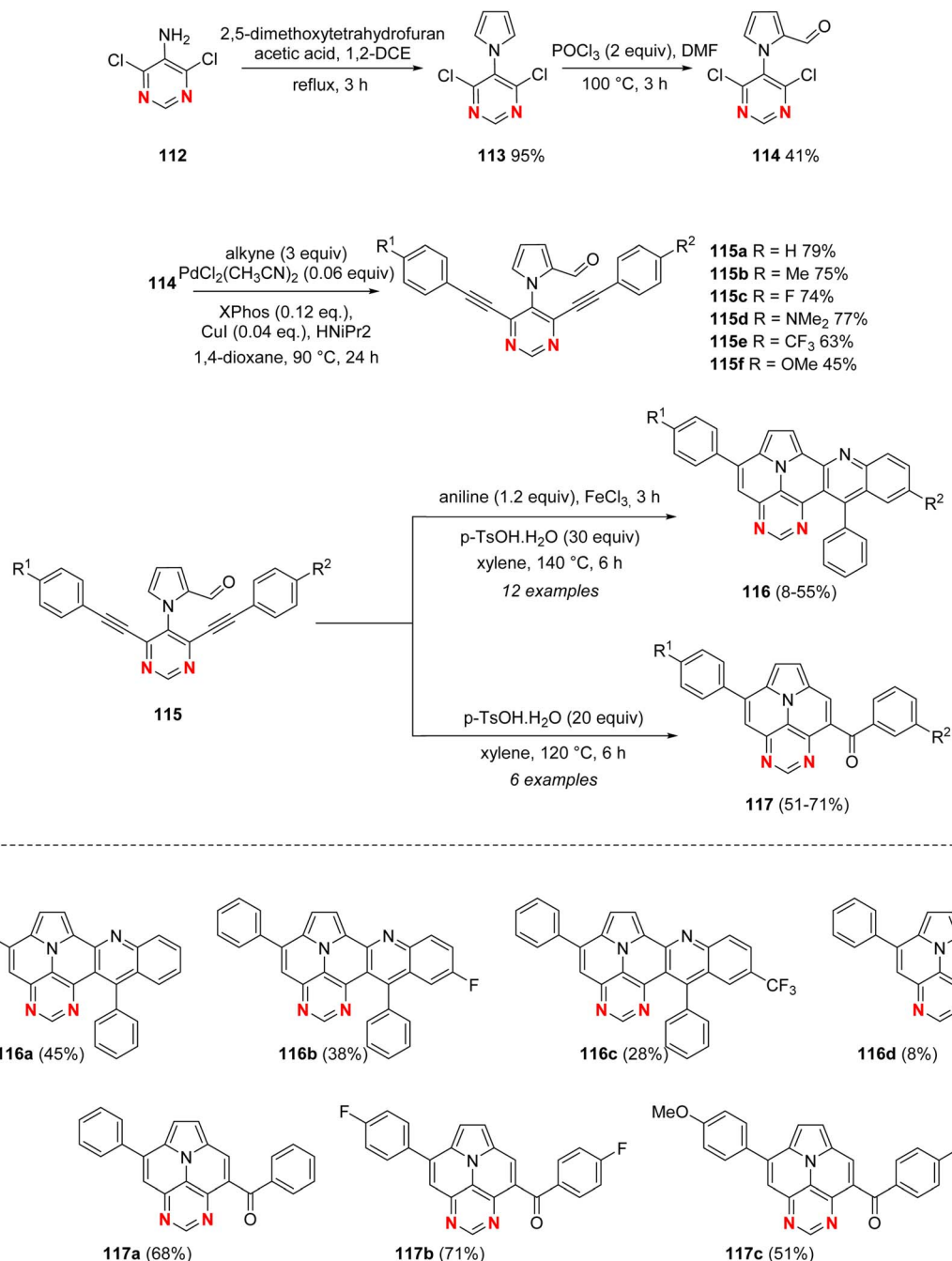
experiments, and DFT calculations. Altogether, the data suggests that the molecular architecture of these aza-ullazines enables fine-tuning of optoelectronic properties, highlighting this class as promising candidates for functional materials applications.

Concurrently, the same research group proposed a divergent strategy for the synthesis of  $\pi$ -expanded diaza-ullazines, exploring two distinct pathways from a single functionalized precursor.<sup>25</sup> The synthetic route begins with a Clausson–Kaas reaction between 4,6-dichloropyrimidine-5-amine **112** and 2,5-dimethoxytetrahydrofuran, affording the pyrrolopyrimidine **113** in excellent yield. Subsequently, a Vilsmeier–Haack reaction was selectively applied to the pyrrole ring, generating the 2-formyl isomer in 41% yield. This compound was then subjected to double Sonogashira couplings with arylacetylenes using  $\text{InCl}_3$ , a widely adopted strategy for promoting annulation *via* intramolecular aromatic substitution of dialkynyl-*N*-(het)arylpyrrole derivatives involved the use of *p*-toluenesulfonic acid (*p*TSA) at elevated temperatures in aromatic hydrocarbon solvents. Beyond its lower cost, *p*TSA demonstrated superior efficiency compared to Lewis acids in several of the mentioned protocols. Moreover, a significant class of unsymmetrical aza-ullazines was accessed in broad substrate scope and with good to excellent yields through a sequence starting from dialkynyl-*N*-(het)arylpyrroles, involving Friedel–Crafts acylation with different anhydrides followed by an intramolecular alkynyl–carbonyl metathesis (ACM) reaction catalyzed by  $\text{Cu}_2\text{CO}_3(\text{OH})_2/\text{K}_2\text{CO}_3$ .

In contrast, the ACM route was optimized using 20 equiv. of *p*-TsOH in xylene at  $120\text{ }^\circ\text{C}$  for 6 hours, providing compound **117a** in 68% yield. Substrate scope evaluation revealed that electron-donating (*e.g.*,  $\text{NMe}_2$ ) and electron-withdrawing (*e.g.*,  $\text{CF}_3$ ) substituents hindered the formation of Povarov-type products, favoring the ACM pathway. Additionally, *o*-substitution on the aniline ring introduced steric effects that reduced cycloaddition efficiency. This synthetic strategy enables rational access to various functionalized diaza-ullazine cores, with promising potential for applications in optoelectronic devices due to their tunable absorption, fluorescence, and redox properties (Scheme 30).

For the synthesis of aza-ullazine derivatives, in addition to Lewis acid-mediated protocols employing reagents such as  $\text{InCl}_3$ , a widely adopted strategy for promoting annulation *via* intramolecular aromatic substitution of dialkynyl-*N*-(het)arylpyrrole derivatives involved the use of *p*-toluenesulfonic acid (*p*TSA) at elevated temperatures in aromatic hydrocarbon solvents. Beyond its lower cost, *p*TSA demonstrated superior efficiency compared to Lewis acids in several of the mentioned protocols. Moreover, a significant class of unsymmetrical aza-ullazines was accessed in broad substrate scope and with good to excellent yields through a sequence starting from dialkynyl-*N*-(het)arylpyrroles, involving Friedel–Crafts acylation with different anhydrides followed by an intramolecular alkynyl–carbonyl metathesis (ACM) reaction catalyzed by  $\text{Cu}_2\text{CO}_3(\text{OH})_2/\text{K}_2\text{CO}_3$ .





Scheme 30 Synthesis of 5,7-diaza-ullazines derivatives.

## 4. Others N-doped ullazines

In the same way that the insertion of a nitrogen atom positively influenced the optoelectronic properties in organic materials derived from aza-ullazines, other N-doped derivatives have been obtained in recent years. These protocols make use of precursors containing imidazole and pyrazole core, being obtained *via* rhodium-catalyzed, together with copper or silver reagents. In 2016, Ge and coworkers<sup>26</sup> reported the synthesis of substituted benzo[*ij*]imidazo[2,1,5-*de*]quinolizines **120a-h** by rhodium(III)-catalyzed multiple C-H activation and annulations. The

reaction occurs *via* cascade oxidative annulation using *N*-aryl-substituted imidazoles **118** with alkynes (2 equiv.) **119** in the presence of [Cp\**Rh*Cl<sub>2</sub>]<sub>2</sub> (5 mol%) and Cu(OAc)<sub>2</sub>·H<sub>2</sub>O (4.0 equiv.) in toluene at 110 °C under argon atmosphere. By this method, twenty one polycyclic heteroaromatic molecules containing benzo[*ij*]imidazo[2,1,5-*de*]quinolizine scaffolds **120a-h** were obtained after 12 h in low to excellent yields (5–99%). The method was shown to be general and was not sensible to the presence of electron-withdrawing and electron-donor groups attached to the aromatic rings of both the alkynyl arene and the *N*-aryl imidazole portions. However, the reaction between the





Scheme 31 Synthesis of substituted benzolijimidazo[2,1,5-de]-quinolizine.

aryl imidazole precursor containing the *p*-NO<sub>2</sub> group and the alkyne resulted in the desired product in only 5% yield, the only limitation of the method. The reaction was also tolerant to heteroaryl and alkyl groups directly bonded to the alkyne, producing the desired compounds **120g** and **120h** in 27% and 63% yields, respectively (Scheme 31). The synthesized molecules exhibit extended  $\pi$ -conjugated systems, essential characteristics for applications in functional organic materials. Their optoelectronic properties, including light absorption and emission, suggest potential applications in organic electronic devices such as solar cells and OFETs. Moreover, their tolerance to diverse functional groups enables targeted structural modifications, broadening their applications in developing novel materials for organic electronics and pharmaceuticals. The

study emphasizes the versatility of these compounds and their significance for advancements in materials science.

The other methods described the generation of cationic species of nitrogenous ullazines such as the method described in 2015 by Ghorai and Choudhury in the synthesis of polycyclic heteroaromatic molecules containing imidazolium scaffolds (Scheme 32).<sup>27</sup>

In this study, the authors have addressed a novel use of N-heterocyclic carbenes (NHCs) for the first time in rhodium(III)-catalyzed double aromatic C–H cascade activation-annulation using readily available imidazolium substrates. The process involves two consecutive C–H activation reactions followed by sequential annulations *via* functionalization of the Rh–CNHC/Rh–caryl bond with internal alkynes **122** to construct a variety of



Scheme 32 Synthesis of benzolijimidazo[2,1,5-de]-quinolizinium scaffolds.





factors such as solvent, substrate, and alkyne used, providing versatile routes for the construction of complex heterocyclic structures. These products have potential applications in the development of new pharmaceuticals and functional materials, owing to their structural diversity and the atom-economical efficiency of the synthetic method, which avoids pre-functionalization steps.

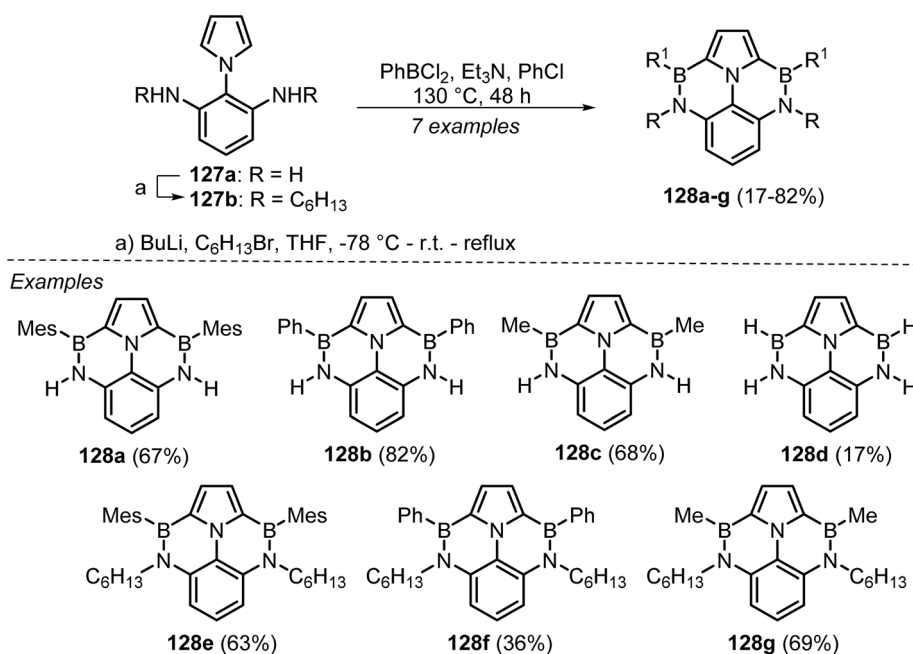
In this section, recent advances in the synthesis of N-doped ullazine derivatives, particularly those incorporating imidazole and pyrazole cores, have expanded the structural and functional diversity of this class of  $\pi$ -conjugated heteroaromatic systems. Rhodium(III)-catalyzed cascade C–H activation/annulation protocols, often combined with copper or silver co-catalysts, have enabled the efficient construction of highly substituted benzo[*ij*]imidazo[2,1,5-*de*]quinolizine, imidazolium, and pyrazolium scaffolds with broad functional group tolerance and variable electronic properties. The resulting compounds exhibit promising optoelectronic characteristics, including strong fluorescence and extended conjugation, making them attractive candidates for applications in organic electronics, photonics, sensors, and pharmaceuticals.

## 5. BO/BN/BS-doped ullazines

An important approach to tune the properties of PAHs is to integrate heteroatoms directly into the  $\pi$ -skeleton. Among these, BN-PAHs can be obtained by replacing the CC unit in PAHs with an isoelectronic and isosteric BN/BO/BS unit. The arrangement, quantity, and orientation of BN units in  $\pi$ -conjugated systems with multiple BN units can significantly affect their electronic and intermolecular properties. The coordination pattern of boron atoms in these systems can further adjust their optoelectronic characteristics, making  $\pi$ -

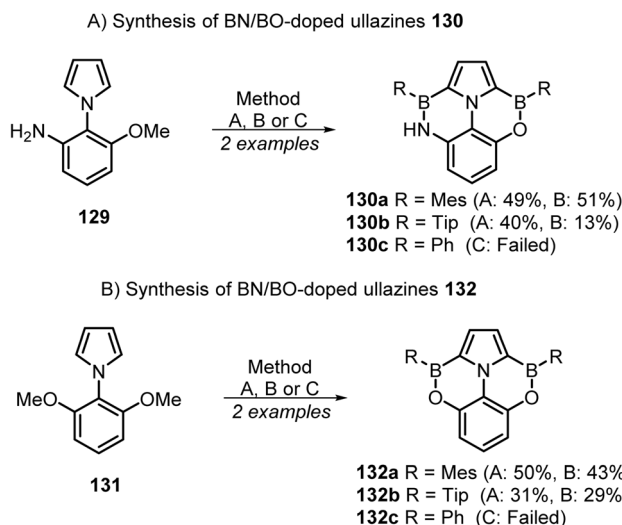
conjugated systems doped with multi-BN promising applications in the field of photonics.<sup>29</sup> In this context, in 2018, Li and coworkers described, according to them, the first synthesis of BN-ullazines (Scheme 35). The synthesis was based in dual Friedel–Crafts-type electrophilic borylation reaction in which two boron atoms are bonded to a central pyrrole.<sup>30</sup> For the synthesis of bis-BN ullazine using substrates **127**, a Clauson–Kaas reaction between 2,5-dimethoxytetrahydrofuran and commercially available 2,6-dinitroaniline was performed, followed by reduction of the NO<sub>2</sub> group to give 2-(1*H*-pyrrol-1-yl)benzene-1,3-diamine, and finally an alkylation using <sup>*n*</sup>BuLi and bromohexane. Bis-BN-ullazines **128a–g** were obtained by consecutive borylative cyclizations of **127a** or **127b** in moderate to good yields in the absence of a catalyst using dichlorophenylborane. However, the authors report a limitation in the method for bis-BN-ullazine **127d**, which is extremely unstable to silica gel chromatography, decomposing slowly during recrystallization, obtained in only 17% yield. The photophysical properties of bis-BN-ullazines, such as blue shifts in their absorption and emission spectra compared to their all-carbon analogs, suggest potential applications in optoelectronic materials, including OLEDs, DSSCs, and OPVs. Furthermore, their unique electronic structure and synthetic accessibility make them promising candidates for the development of new functional materials with tunable properties for applications in organic electronics and sensors.

Another possibility involves the synthesis of BO-PAH derivatives (Scheme 36). In this context, oxygen's higher electronegativity compared to nitrogen leads to PAHs with more polar B–O bonds, often resulting in distinct aromatic properties. Following this approach, Guo and coworkers<sup>31</sup> reported the synthesis of BN/BO-doped ullazines **130** and **132**. The substrates **129** and **131** used were synthesized by the Clauson–Kaas



Scheme 35 Synthesis of bis-BN ullazines.



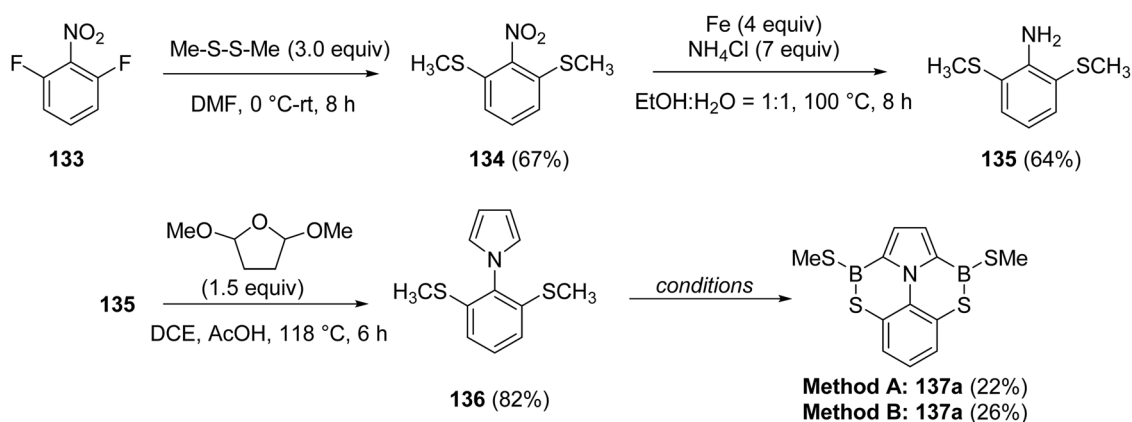


**Scheme 36** Synthesis of BN/BO-doped ullazines. Method A (R = Mes, Tip):  $\text{BCl}_3$ ,  $\text{Et}_3\text{N}$ ,  $\text{Bu}_4\text{NI}$ ,  $\text{PhCl}$ ,  $135^\circ\text{C}$ , 24 h. Then  $\text{RMgBr}$ , r.t., 5–24 h; method B (R = Mes, Tip):  $\text{BBr}_3$ , *o*-DCB, r.t., 20 h. Then  $\text{TMP}$ ,  $180^\circ\text{C}$ , 18 h. Then  $\text{RMgBr}$ , r.t., 4–24 h; method C (R = Ph):  $\text{PhBCl}_2$ ,  $\text{Et}_3\text{N}$ ,  $\text{Bu}_4\text{NI}$ ,  $\text{PhCl}$ ,  $135^\circ\text{C}$ , 24 h.

reaction between 2-methoxy-6-nitroaniline and 2,5-dimethoxytetrahydrofuran, followed by a reduction of the nitro group using iron. Nitrogen-directed demethylation and borylation proceeded smoothly to yield the BN/BO-doped ullazines (Scheme 36A). However, a phenyl substituent on boron was not effective to afford **130c**, while stable BN/BO-ullazines **130a** and **130b** were isolated and purified with the Mes (mesityl) or Tip (triisopropylphenyl) Grignard reagent as nucleophile. Bis-BO-ullazines **132** were prepared using 1-(2,6-dimethoxyphenyl)-1*H*-pyrrole **131** as the main borylation precursor (Scheme 36B). Obtained by Clauson–Kaas reaction between 2,6-dimethoxyaniline and 2,5-dimethoxytetrahydrofuran. Similarly, **132c** could not be obtained, while **132a** and **132b** are stable

enough for chromatography on neutral alumina but not stable on silica gel. The synthesized compounds exhibit structural planarity, tunable aromaticity, and favorable frontier energy levels for n-type semiconductor materials. Additionally, they demonstrate UV-region emission with significant quantum yields, making them promising candidates for use in UV-OLEDs. The study also explores the influence of BO doping on electronic and photophysical properties, laying the groundwork for future applications in organic electronics and photonic devices.

Recently, Popp and coworkers,<sup>32</sup> described the synthesis of a novel bis-boron/sulfur-doped ullazine (Bis-BS-U), contributing to the growing interest in heteroatom-doped  $\pi$ -conjugated systems for optoelectronic applications. The synthetic strategy was designed to build the B,S-doped framework through a sequence of well-defined steps, beginning with a nucleophilic aromatic substitution between commercially available 2,6-difluoronitrobenzene **133** and 1,2-dimethyldisulfane. This reaction yielded (2-nitro-1,3-phenylene)bis(methylsulfane), which was then reduced using iron powder under acidic conditions to furnish 2,6-bis(methylthio)aniline **134**. The resulting aniline derivative underwent a Clauson–Kaas pyrrole-forming reaction with 2,5-dimethoxytetrahydrofuran, affording the key ullazine precursor in excellent yield (82%). The final step involved a three-part sequence: demethylation, borylation, and nucleophilic substitution, which introduced two boron centers flanked by mesityl groups. Boron tribromide ( $\text{BBr}_3$ ) served as both the demethylating and borylating agent. Without additives (Method A), the reaction proceeded at  $180^\circ\text{C}$  and yielded Bis-BS-U in 22% after trapping with mesityl Grignard reagent. In the optimized procedure (Method B), the addition of tetrabutylammonium iodide allowed the reaction to proceed at a lower temperature ( $135^\circ\text{C}$ ), increasing the yield to 26% (Scheme 37). The final compound exhibited excellent chemical and thermal stability, withstanding air and moisture, and was readily purified by flash chromatography. Thermogravimetric analysis (TGA) revealed a 5% mass loss only at  $282^\circ\text{C}$ ,



A)  $\text{BBr}_3$ , *o*-DCB,  $180^\circ\text{C}$ ;  $\text{Et}_3\text{N}$ ,  $180^\circ\text{C}$ , 24 h, Then  $\text{RMgBr}$ , rt, 12 h  
B)  $\text{BBr}_3$ ,  $\text{Et}_3\text{N}$ ,  $\text{Bu}_4\text{NI}$ ,  $\text{PhCl}$ ,  $135^\circ\text{C}$ , 24 h, Then  $\text{RMgBr}$ , rt, 12 h

**Scheme 37** Synthesis of BS-doped ullazines **137a**.



highlighting the thermal robustness of Bis-BS-U. These properties, along with its unique BS doping pattern, support its potential for use in organic electronics.

Thus, the incorporation of BN, BO, and BS units into ullazine frameworks offers a powerful strategy to modulate their electronic structure, photophysical behavior, and stability, enabling access to materials with tunable properties for optoelectronic applications. These methodologies generally exhibit good functional group tolerance, allow structural diversification, and in many cases avoid the need for metal catalysts, aligning with green chemistry principles. However, some derivatives display limited stability, particularly toward silica gel chromatography, and certain substitution patterns remain inaccessible, leading to reduced yields or complete reaction failure. Additionally, the multi-step synthetic sequences and moderate overall yields for specific doped systems highlight the need for further optimization to improve scalability and broaden substrate scope.

## 6. Ullazines fused to another heterocycle

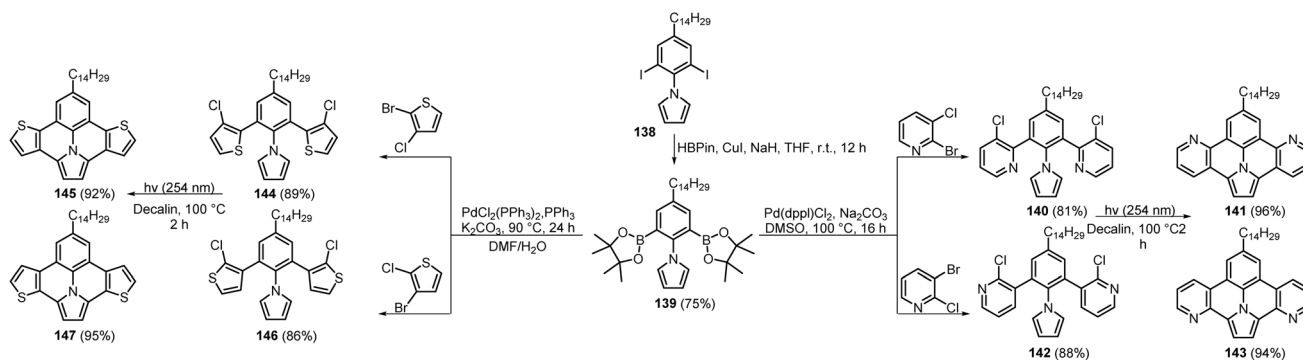
In addition to the methods already described throughout this review, some researchers have reported synthesis protocols for ullazine scaffolds containing heterocycles in different portions of the core. In 2019, Miao and coworkers<sup>33</sup> described an approach for the synthesis of ullazine derivatives that involved the photochemical cyclodehydrochlorination (CDHC) reaction as the main step (Scheme 38). For this, compound **138** was obtained by the following steps: iodination at 2- and 6-positions of 4-tetradecylaniline using iodine monochloride in a mixture of water and hydrochloric acid; and formation of pyrrole by Clauson-Kass reaction and 2,5-dimethoxytetrahydrofuran in the mixture of AcOH and 1,2-dichloroethane. Then, the obtained compound **138** was subjected to a double borylation reaction using copper iodide (CuI) as catalyst to give compound **139** in 75% yield. Finally, it was subjected to a coupling reaction with 2-bromo-3-chloropyridine and 3-bromo-2-chloropyridine using Pd(dppf)Cl<sub>2</sub> as catalyst to give compounds **140** and **142** in good yields (81 and 88%). Similarly, coupling with 2-bromo-3-chlorothiophene and 3-bromo-2-chlorothiophene using PdCl<sub>2</sub>(PPh<sub>3</sub>)<sub>2</sub> as catalyst was carried out to give compounds **144** and **146** in 89 and 86% yield, respectively. These obtained

derivatives were subjected to a photochemical cyclodehydrochlorination (CDHC) reaction using the chlorinated precursors dissolved in degassed decahydronaphthalene at a concentration of 0.001 M and the solutions were irradiated under UV light (16 × 7.2 W low-pressure mercury lamps, λ = 254 nm) at 100 °C for 2 h under a continuous flow of argon. By this method, the photocyclized compounds **141**, **143**, **145** and **147** were obtained in excellent yields (94–96%). Furthermore, one of the thiophene-fused **147** was copolymerized with different electron-deficient moieties obtaining **149a–c** in excellent yields (89–92%, Scheme 39). According to the authors, these D–A conjugated polymers were reported for the first time and tested in bulk heterojunction solar cells with promising results.

The most electron-donating compound was copolymerized with acceptor units – thienopyrroledione (TPD), isoindigo (IID) and diketopyrrolopyrrole (DPP) – to form donor–acceptor (D–A) conjugated polymers. These polymers exhibited broad UV-vis-NIR absorption bands, with optical gaps ranging from 1.24 eV to 1.58 eV, suitable for solar cell applications. Bulk heterojunction photovoltaic devices (BHJ-PSCs) were fabricated, achieving a PCE of up to 2.23%. The work demonstrates the potential of ullazine derivatives as efficient building blocks for organic semiconductor materials in solar energy, highlighting their versatility and tunable electronic properties.

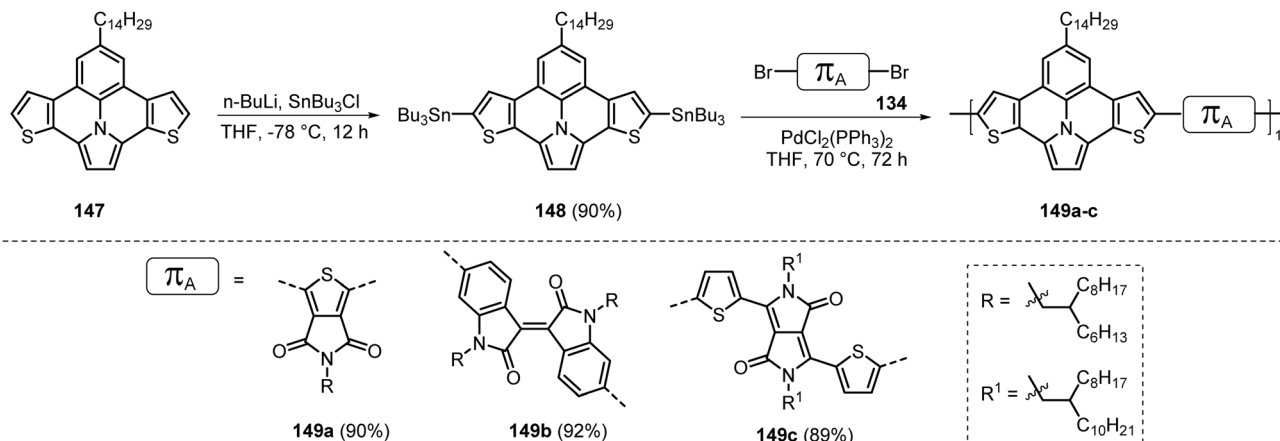
In a more recent protocol, Dumele and coworkers<sup>34</sup> described the synthesis of supramolecular polymer scaffolds that integrate light-absorbing chromophores and catalysts into materials for light-driven CO<sub>2</sub> reduction. The authors reported that this was a groundbreaking study of the self-assembly of ullazine derivatives into supramolecular structures. Specific modifications were introduced to optimize the performance of the ullazine core. A chromophore amphiphile was created by attaching a mono-imide group with carboxylic acid *via* a five-carbon linker. This imide group conferred a dipole moment to the π-extended core, while the carboxylate functioned as an ionizable hydrophilic head in water. Also, the ullazine core was extended laterally to enhance visible light absorption. Finally, an *n*-pentyl group was added on the side opposite the hydrophilic vector to increase molecular solubility during synthesis and support further hydrophobic self-assembly.

For the synthesis of compounds **153** and **157** the authors described an adaptation of the selective 1,3-dipolar



Scheme 38 Synthetic routes of ullazine derivatives.





Scheme 39 Synthetic routes to the D–A polymers.

cycloaddition reaction between azomethine ylide and dipolarophile *tert*-butyl 6-maleimido-hexanoate. Initially, diol **150** was subjected to HCl-induced microwave-assisted cyclization and oxidation by trityl tetrafluoroborate. According to the authors, for dithienoazomethine ylide **155**, the preparation of diol **154** had to account for the inherent instability of 2-thienylboronic acid by exploiting its *in situ* slow-release cross-coupling of the corresponding trivalent *N*-methyliminodiacetic acid (MIDA) boronate. These two azomethine ylide precursors (**151** and **155**) were subjected to one-pot 1,3-dipolar cycloaddition reactions with *tert*-butyl 6-maleimido-hexanoate, followed

by oxidation/rearomatization of the cycloaddition intermediates with 2,3-dichloro-5,6-dicyano-1,4-benzoquinone (DDQ). By this method, the *tert*-butyl esters were obtained and quantitatively deprotected using trifluoroacetic acid. In summary, monomers amphiphilic chromophores with a diene-fused ullazine core that self-assemble into supramolecular polymers in water, forming entangled nanoscale fibers. When exposed to visible light at 450 nm, these fibers activate a dinuclear cobalt catalyst for the photoreduction of CO<sub>2</sub>, producing carbon monoxide and methane with the help of a sacrificial electron donor. This supramolecular photocatalytic system achieves CH<sub>4</sub>



**Scheme 40** Synthesis of supramolecular polymer scaffolds. Conditions: (a) (step i) HCl (4 M in 1,4-dioxane), MW, 130 °C, N<sub>2</sub>; (step ii) CPh<sub>3</sub>BF<sub>4</sub>, CH<sub>3</sub>CN/toluene, 90 °C, N<sub>2</sub>; (b) (step i) *t*butyl 6-maleimido-hexanoate, Et<sub>3</sub>N, CH<sub>2</sub>Cl<sub>2</sub>, 25 °C, N<sub>2</sub>; (step ii) DDQ, CH<sub>2</sub>Cl<sub>2</sub>/toluene, 25 °C, N<sub>2</sub>; (c) CF<sub>3</sub>CO<sub>2</sub>H, CH<sub>2</sub>Cl<sub>2</sub>, 25 °C.



yields comparable to those from the precious metal-based [Ru(phen)<sub>3</sub>](PF<sub>6</sub>)<sub>2</sub> sensitizer and, in contrast to Ru-based catalysts, maintains photocatalytic performance in aqueous environments for over six days (Scheme 40).

These compounds self-assemble into nanofibers that, upon visible light irradiation (450 nm), sensitize dinuclear cobalt catalysts (CoCo-1 and CoCo-2), enabling the conversion of CO<sub>2</sub> into CO and CH<sub>4</sub> with efficiencies comparable to those of ruthenium (Ru)-based systems. Notably, the supramolecular polymers exhibited prolonged stability (up to 6 days) and sustained activity in fully aqueous media, addressing key limitations of conventional metal-based photosensitizers. This work underscores the potential of these materials as sustainable alternatives for solar fuel production and CO<sub>2</sub> mitigation, with promising applications in renewable energy and carbon capture and conversion technologies.

In summary, these methodologies highlight the versatility of ullazine derivatives as building blocks for advanced functional materials, offering high synthetic yields, structural tunability, and compatibility with diverse heterocyclic units. Photochemical strategies enable efficient and catalyst-free cyclizations, while supramolecular self-assembly approaches expand their applicability to sustainable photocatalysis and solar energy conversion. Advantages include broad optoelectronic tunability, high performance in aqueous media, and potential for renewable energy applications. However, certain protocols require multi-step reactions, specialized photochemical setups, or sensitive intermediates, which may limit scalability.

## 7. Conclusion

Recent advances in the synthetic chemistry of ullazines have led to a broad spectrum of structurally diverse and electronically tunable derivatives. The development of modular and efficient methods, including InCl<sub>3</sub>-promoted annulations, photochemical cyclizations, and metal-catalyzed C–H activation, has enabled access to  $\pi$ -extended frameworks with high regioselectivity and functional group tolerance. Emerging strategies, such as visible-light photocatalysis and cascade cyclizations, further expand structural diversity and allow precise heteroatom incorporation (e.g., N, B, O, S). These innovations have positioned ullazine-based systems as versatile platforms for the design of functional materials in organic electronics, particularly in light-harvesting applications such as DSSCs, PSCs, and photocatalytic systems. The continued evolution of synthetic approaches is expected to unlock new opportunities in the development of high-performance optoelectronic devices.

## Conflicts of interest

There are no conflicts to declare.

## Data availability

The data used in this study are publicly available and can be accessed through online repositories and the journals where the

study was published. There are no specific restrictions or conditions for accessing the data.

## Acknowledgements

Fellowships granted by CNPq (404587/2021-6, 310656/2021-4, 402854/2023-3 and 306952/2025-4), CAPES (Funding Code 001), and FAPERJ are gratefully acknowledged. We are indebted to the support given by the FAPERJ – Process E-26/211.343/2021, E-26/210.333/2022, E-26/210.325/2022, E-26/200.235/2023, and 26/204.583/2024.

## References

- C. Cebrián, Ullazine-Based Materials: Towards Novel Opportunities in Organic Electronics, *J. Mater. Chem. C*, 2018, **6**(44), 11943–11950, DOI: [10.1039/c8tc03573c](https://doi.org/10.1039/c8tc03573c).
- (a) M. Stepien, E. Gońka, M. Żyła and N. Sprutta, Heterocyclic Nanographenes and Other Polycyclic Heteroaromatic Compounds: Synthetic Routes, Properties, and Applications, *Chem. Rev.*, 2017, **117**(4), 3479–3716, DOI: [10.1021/acs.chemrev.6b00076](https://doi.org/10.1021/acs.chemrev.6b00076); (b) P. Langer, Palladium-Catalyzed Synthesis of Heterocyclic Ring Systems by Combination of Regioselective C–C with Twofold C–N Couplings, *Synlett*, 2022, **33**(13), 1215–1226, DOI: [10.1055/s-0040-1719918](https://doi.org/10.1055/s-0040-1719918); (c) P. Langer, Synthesis of Heterocycles by a C–C Cross-Coupling/Alkyne-Carbonyl-Metathesis Strategy, *Synlett*, 2024, **35**(17), 1965–1975, DOI: [10.1055/s-0042-1751513](https://doi.org/10.1055/s-0042-1751513).
- J. H. Delcamp, A. Yella, T. W. Holcombe, M. K. Nazeeruddin and M. Grätzel, The Molecular Engineering of Organic Sensitizers for Solar-Cell Applications, *Angew. Chem., Int. Ed.*, 2013, **52**(1), 376–380, DOI: [10.1002/anie.201205007](https://doi.org/10.1002/anie.201205007).
- Z. Shao, Y. Wang, H. Wang, P. Cui and X. Liu, Recent Advance in the Synthesis of Ullazine and Its Derivatives, *Chin. J. Org. Chem.*, 2023, **43**, 3679–3694, DOI: [10.6023/cjoc202306020](https://doi.org/10.6023/cjoc202306020).
- D. Miao, C. Aumaitre and J. F. Morin, Photochemical Synthesis of  $\pi$ -Extended Ullazine Derivatives as New Electron Donors for Efficient Conjugated D-A Polymers, *J. Mater. Chem. C*, 2019, **7**(10), 3015–3024, DOI: [10.1039/c8tc05288c](https://doi.org/10.1039/c8tc05288c).
- (a) H. Balli and M. Zeller, Neue Heteroarene: Synthese und spektrale Daten von Indolizino[6,5,4,3-*aij*]chinolin ( $\llcorner$ Ullazin $\gg$ ) und einigen Derivaten, *Helvetica Chim. Acta*, 1983, **66**(7), 2135–2139, DOI: [10.1002/hlca.19830660724](https://doi.org/10.1002/hlca.19830660724); (b) K.-i. Kanno, Y. Liu, A. Iesato, K. Nakajima and T. Takahashi, Chromium-Mediated Synthesis of Polycyclic Aromatic Compounds from Halobiaryls, *Org. Lett.*, 2005, **7**(24), 5453–5456, DOI: [10.1021/ol052214x](https://doi.org/10.1021/ol052214x).
- J. H. Delcamp, A. Yella, T. W. Holcombe, M. K. Nazeeruddin and M. Grätzel, The Molecular Engineering of Organic Sensitizers for Solar-Cell Applications, *Angew. Chem., Int. Ed.*, 2012, **52**(1), 376–380, DOI: [10.1002/anie.201205007](https://doi.org/10.1002/anie.201205007).
- P. Pierrat, S. Hesse, C. Cebrián and P. C. Gros, Controlling charge-transfer properties through a microwave-assisted mono- or bis-annulation of dialkynyl-*N*-(het)arylpyrroles,



- Org. Biomol. Chem.*, 2017, **15**(40), 8568–8575, DOI: [10.1039/c7ob02149f](https://doi.org/10.1039/c7ob02149f).
- 9 N. A. Drigo, S. Paek, A. J. Huckaba, P. A. Schouwink, N. Tabet and M. K. Nazeeruddin, Approaches for Selective Synthesis of Ullazine Donor-Acceptor Systems, *Chem.–Eur. J.*, 2017, **23**(68), 17209–17212, DOI: [10.1002/chem.201704694](https://doi.org/10.1002/chem.201704694).
- 10 H. Qiao, Y. Deng, R. Peng, G. Wang, J. Yuan and S. Tan, Effect of  $\pi$ -spacers and anchoring groups on the photovoltaic performances of ullazine-based dyes, *RSC Adv.*, 2016, **6**(74), 70046–70055, DOI: [10.1039/c6ra11918b](https://doi.org/10.1039/c6ra11918b).
- 11 Y. Zhang, H. Cheema, L. McNamara, L. A. Hunt, N. I. Hammer and J. H. Delcamp, Ullazine Donor- $\pi$  bridge-Acceptor Organic Dyes for Dye-Sensitized Solar Cells, *Chem.–Eur. J.*, 2018, **24**(22), 5939–5949, DOI: [10.1002/chem.201800030](https://doi.org/10.1002/chem.201800030).
- 12 L. Q. Bao, S. Thogiti, G. Koyyada and J. H. Kim, Synthesis and photovoltaic performance of novel ullazine-based organic dyes for dye-sensitized solar cells, *Jpn. J. Appl. Phys.*, 2019, **58**(1), 012011, DOI: [10.7567/1347-4065/aaf2d1](https://doi.org/10.7567/1347-4065/aaf2d1).
- 13 G. Zhang, P. Gautam and J. M. W. Chan, Symmetrical and unsymmetrical fluorine-rich ullazines *via* controlled cycloaromatizations, *Org. Chem. Front.*, 2020, **7**(5), 787–795, DOI: [10.1039/d0qo00033g](https://doi.org/10.1039/d0qo00033g).
- 14 J. Xia, M. Cavazzini, C. Igci, C. Momblona, S. Orlandi, B. Ding, Y. Zhang, H. Kanda, N. Klipfel, S. B. Khan, *et al.*, Molecular Engineering of Thienyl Functionalized Ullazines as Hole-Transporting Materials for Perovskite Solar Cells, *Sol. RRL*, 2021, **6**(4), 2100926, DOI: [10.1002/solr.202100926](https://doi.org/10.1002/solr.202100926).
- 15 D. Wan, X. Li, R. Jiang, B. Feng, J. Lan, R. Wang and J. You, Palladium-Catalyzed Annulation of Internal Alkynes: Direct Access to  $\pi$ -Conjugated Ullazines, *Org. Lett.*, 2016, **18**(12), 2876–2879, DOI: [10.1021/acs.orglett.6b01182](https://doi.org/10.1021/acs.orglett.6b01182).
- 16 D. Wang, Y. Liu, L. Wang, H. Cheng, Y. Zhang and G. Gao, Synthesis of  $\pi$ -extended dibenzo[*d,k*]ullazines by a palladium-catalyzed double annulation using arynes, *Chin. Chem. Lett.*, 2021, **32**(4), 1407–1410, DOI: [10.1016/j.ccl.2020.09.057](https://doi.org/10.1016/j.ccl.2020.09.057).
- 17 S. Otero Riesgo, J. A. Varela and C. Saá, One-Pot Rh(III)-Catalyzed Twofold C-H Activation/Oxidative Annulation of N-Arylpyrroles with Alkynes to Fluorescent Ullazines, *Adv. Synth. Catal.*, 2024, **366**(10), 2312–2323, DOI: [10.1002/adsc.202400043](https://doi.org/10.1002/adsc.202400043).
- 18 A. Das, I. Ghosh and B. König, Synthesis of pyrrolo[1,2-*a*]quinolines and ullazines by visible light mediated one- and twofold annulation of *N*-arylpyrroles with arylalkynes, *Chem. Commun.*, 2016, **52**(56), 8695–8698, DOI: [10.1039/c6cc04366f](https://doi.org/10.1039/c6cc04366f).
- 19 T. J. Peglow, P. C. Nobre, J. P. S. S. C. Thomaz, M. M. Vieira, H. C. S. Junior, B. T. Dalberto, P. H. Schneider, F. S. Rodembusch and V. Nascimento, Synthesis and Photophysical Evaluation of Dialkynyl-*N*-(het)arylpyrroles: A Promising Key Compounds in Fluorescence Chemistry, *Asian J. Org. Chem.*, 2024, **13**(4), e202300655, DOI: [10.1002/ajoc.202300655](https://doi.org/10.1002/ajoc.202300655).
- 20 S. Boldt, S. Parpart, A. Villinger, P. Ehlers and P. Langer, Synthesis and properties of aza-ullazines, *Angew. Chem.*, 2017, **129**, 4646–4649; S. Boldt, *Angew. Chem., Int. Ed.*, 2017, **56**(16), 4575–4578, DOI: [10.1002/anie.201701347](https://doi.org/10.1002/anie.201701347).
- 21 S. Janke, S. Boldt, P. Nakielski, A. Villinger, P. Ehlers and P. Langer, Synthesis and Properties of 5-Azaullazines, *J. Org. Chem.*, 2023, **88**(15), 10470–10482, DOI: [10.1021/acs.joc.3c00386](https://doi.org/10.1021/acs.joc.3c00386).
- 22 S. Parpart, S. Boldt, P. Ehlers and P. Langer, Synthesis of Unsymmetrical Aza-Ullazines by Intramolecular Alkynyl-Carbonyl Metathesis, *Org. Lett.*, 2017, **20**(1), 122–125, DOI: [10.1021/acs.orglett.7b03477](https://doi.org/10.1021/acs.orglett.7b03477).
- 23 D. Ibrahim, P. Boulet, P. C. Gros and P. Pierrat, Efficient Access to Arylated Aza-ullazines by Regioselective Functionalization of their Pyridine Ring by H–Li Exchange and Electrophilic Substitution, *Eur. J. Org. Chem.*, 2021, **2021**(22), 3331–3339, DOI: [10.1002/ejoc.202100333](https://doi.org/10.1002/ejoc.202100333).
- 24 J. Polkaehn, R. Thom, P. Ehlers, A. Villinger and P. Langer,  $\pi$ -expanded azaullazines: synthesis of quinolino-azaullazines by Povarov reaction and cycloisomerisation, *Org. Biomol. Chem.*, 2024, **22**, 2027–2042, DOI: [10.1039/d4ob00091a](https://doi.org/10.1039/d4ob00091a).
- 25 J. Polkaehn, P. Ehlers, A. Villinger and P. Langer, Divergent Synthesis of 5,7-Diazaullazines Derivatives through a Combination of Cycloisomerization with Povarov or Alkyne–Carbonyl Metathesis, *Molecules*, 2024, **29**, 2159, DOI: [10.3390/molecules29092159](https://doi.org/10.3390/molecules29092159).
- 26 Q. Ge, B. Li and B. Wang, Synthesis of substituted benzo[*ij*]imidazo[2,1,5-*de*]quinolizine by rhodium(iii)-catalyzed multiple C–H activation and annulations, *Org. Biomol. Chem.*, 2016, **14**(5), 1814–1821, DOI: [10.1039/c5ob02515j](https://doi.org/10.1039/c5ob02515j).
- 27 D. Ghorai and J. Choudhury, Rhodium(III)-N-Heterocyclic Carbene-Driven Cascade C–H Activation Catalysis, *ACS Catal.*, 2015, **5**(4), 2692–2696, DOI: [10.1021/acscatal.5b00243](https://doi.org/10.1021/acscatal.5b00243).
- 28 D. L. Davies, C. E. Ellul, S. A. Macgregor, C. L. McMullin and K. Singh, Experimental and DFT Studies Explain Solvent Control of C–H Activation and Product Selectivity in the Rh(III)-Catalyzed Formation of Neutral and Cationic Heterocycles, *J. Am. Chem. Soc.*, 2015, **137**(30), 9659–9669, DOI: [10.1021/jacs.5b04858](https://doi.org/10.1021/jacs.5b04858).
- 29 X. Chen, D. Tan and D.-T. Yang, Multiple-boron-nitrogen (multi-BN) doped  $\pi$ -conjugated systems for optoelectronics, *J. Mater. Chem. C*, 2022, **10**, 13499–13532, DOI: [10.1039/d2tc01106a](https://doi.org/10.1039/d2tc01106a).
- 30 C. Li, Y. Liu, Z. Sun, J. Zhang, M. Liu, C. Zhang, Q. Zhang, H. Wang and X. Liu, Synthesis, Characterization, and Properties of Bis-BN Ullazines, *Org. Lett.*, 2018, **20**(10), 2806–2810, DOI: [10.1021/acs.orglett.8b00554](https://doi.org/10.1021/acs.orglett.8b00554).
- 31 Y. Guo, L. Zhang, C. Li, M. Jin, Y. Zhang, J. Ye, Y. Chen, X. Wu and X. Liu, BN/BO-Ullazines and Bis-BO-Ullazines: Effect of BO Doping on Aromaticity and Optoelectronic Properties, *J. Org. Chem.*, 2021, **86**(18), 12507–12516, DOI: [10.1021/acs.joc.1c00777](https://doi.org/10.1021/acs.joc.1c00777).
- 32 J. Popp, M. Duser and M. Enders, Synthesis of a bis-boron/sulfur doped ullazine and direct comparison with its boron/nitrogen and boron/oxygen analogues, *Asian J. Org. Chem.*, 2025, **14**(3), e202400637, DOI: [10.1002/ajoc.202400637](https://doi.org/10.1002/ajoc.202400637).



- 33 D. Miao, C. Aumaitre and J.-F. Morin, Photochemical synthesis of  $\pi$ -extended ullazine derivatives as new electron donors for efficient conjugated D–A polymers, *J. Mater. Chem. C*, 2019, 7(10), 3015–3024, DOI: [10.1039/c8tc05288c](https://doi.org/10.1039/c8tc05288c).
- 34 O. Dumele, L. Đorđević, H. Sai, T. J. Cotey, M. H. Sangji, K. Sato, A. J. Dannenhoffer and S. I. Stupp, Photocatalytic Aqueous CO<sub>2</sub> Reduction to CO and CH<sub>4</sub> Sensitized by Ullazine Supramolecular Polymers, *J. Am. Chem. Soc.*, 2022, 144(7), 3127–3136, DOI: [10.1021/jacs.1c12155](https://doi.org/10.1021/jacs.1c12155).

